Institute of High Frequency Technology

RWTH AACHEN UNIVERSITY

Master Thesis

Investigation and Development of an Optimization Technique for Antenna Characterization

David Valencia Gutiérrez

350398

15th April 2015

Supervisors: Prof. Dr.-Ing. Dirk Heberling
M. Sc. Hammam Shakhtour

Ich erkläre hiermit, dass ich diese Arbeit selbständig verfaßt, noch nicht anderweitig für andere Prüfungszwecke vorgelegt, keine anderen als die angegebenen Quellen und Hilfsmittel -- bis auf die offizielle Betreuung durch das Institut für Hochfrequenztechnik -- benutzt sowie wörtliche und sinngemäße Zitate als solche gekennzeichnet habe. Weiterihn erkläre ich mein Einverständnis, dass die RWTH Aachen diese Prüfungsleistung den Studenten und Mitarbeitern der RWTH Aachen zur Einsicht überlassen, sowie als Ganzes oder in Auszügen veröffentlichen darf

Scope of work

The Near-Field Measurements have gained fame in the last years since they offer some advantages. For instance, from the near-field data and by applying a mathematical transformation, the far-field radiation pattern can be constructed. However, it is necessary to have the amplitude and the phase distribution in the near-field to achieve a good reconstruction of the far-field radiation pattern. Due to the problems that the phase measurements present and the fact that, for some particular antennas, phase measurements are non-viable, the reconstruction of the far-field radiation pattern from only amplitude near-field measurements is addressed in this thesis, and different methods and techniques to reconstruct the phase distribution from the amplitude data based on the minimization of a cost function are investigated and developed.

Summary

The goal of this thesis is to reconstruct with a certain level of accuracy the far-field radiation pattern of an antenna from only amplitude near-field measurements The planar configuration was chosen to acquire the amplitude measurements over two scanning planes located few wavelengths away from the antenna aperture. Since the phase is missing in this context, suitable methods have been investigated and developed to reconstruct the phase of the field from the amplitude data. The Fourier Iterative Algorithm has been implemented to reconstruct the phase from the amplitude data but presents the problem of the strong dependence on the initial guess of the field over the antenna aperture.

A Global Optimization technique based on a Genetic Algorithm has been developed to find the initial estimation of the field over the antenna aperture which feeds the iterative technique and the effect of using this global optimization on the accuracy of the reconstructed far-field radiation pattern have been investigated. Apart from that, a technique that combines the Genetic Algorithm and the Fourier Iterative Algorithm has been implemented to reconstruct the phase information from the amplitude data.

For the Horn antenna as the antenna under test it has been found that, by implementing the Global Optimization as the method to find the initial condition for the Fourier Iterative Algorithm, no enhancement on the accuracy of the far-field is found. On the other hand, by applying the second method that combines the Genetic Algorithm and the Fourier Iterative technique the improvement of the accuracy of the reconstructed radiation pattern is finally obtained in the region of the main lobe and the secondary lobes.

Table of contents

Scope of work IV
Summary V
1 Introduction 7
2 Planar Near-Field Antenna Measurements 10
3 The Phase Retrieval Method 17
4 The Genetic Algorithm 31
5 Simulations and Results 44
6 Conclusions 70
7 Future Work 72
List of Figures 73
Bibliography 76

1 Introduction

When we want to characterize an antenna, parameters such as directivity, gain or the far-field radiation pattern are looked for. The reader is recommended [1] for a detailed discussion of these parameters. In this thesis, we are especially focused on the radiation pattern of the antenna.

Basically, the electromagnetic field produced by an antenna can be divided into three different regions, as it is shown in Figure 1.

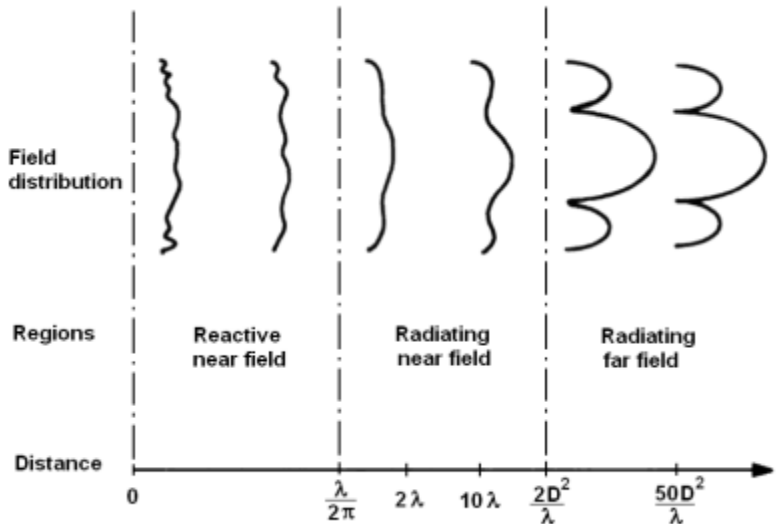

Figure 1: Exterior fields of a radiating antenna [*Reconstruction of the antenna near-field* Jan Puskely, Figure 1.1]

In the closest region to the antenna aperture, the reactive zone, the energy decays rapidly as a function of the distance. Here we have the presence of the evanescent modes. In the radiating near-field zone; near-field measurements are done as we will see in the following chapters. Finally, in the far-field region, we only have propagating fields [1].

In the far-field region an antenna is characterized by illuminating it with a plane wave, i.e., wave with uniform distribution of amplitude and phase. It is hard to accomplish a uniform plane wave, but this phenomenon can be approximated by separating the observer a long distance away from the antenna under test.

On the other hand, in near-field antenna measurements we can measure the field near the antenna aperture. Apart from that, we can find the far-field properties of the antenna directly from the near-field measurements by applying a suitable mathematical transformation, as it is going to be explained in Chapter 2.

In order to achieve a good prediction of the far-field radiation properties of the antenna from the near-field measurements we need both, the amplitude and the phase distribution of the near-field. Then, the near-field to far-field transformation can be made. Figure 2 shows a general diagram of this procedure.

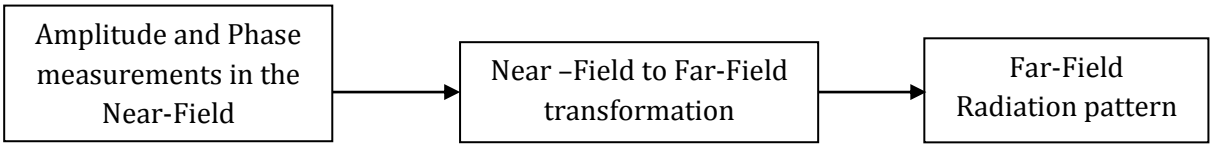

Figure 2: Procedure to reconstruct the far-field from complex near-field measurements.

For some particular antennas, the acquisition of the phase is difficult, or even impossible. In fact, the probe positioning errors of the scanning system result essentially in uncertainties on the detected phase. Furthermore, the phase measurement is quite more sensitive to the equipment inaccuracies [4]. Therefore, the goal of this project is to construct a suitable procedure to reconstruct the phase distribution in the near-field from the amplitude measurements and then, reconstruct the far-field radiation pattern with an acceptable degree of accuracy. The procedure we have to follow to construct the far-field radiation pattern from only-amplitude near-field measurements is described in Figure 3:

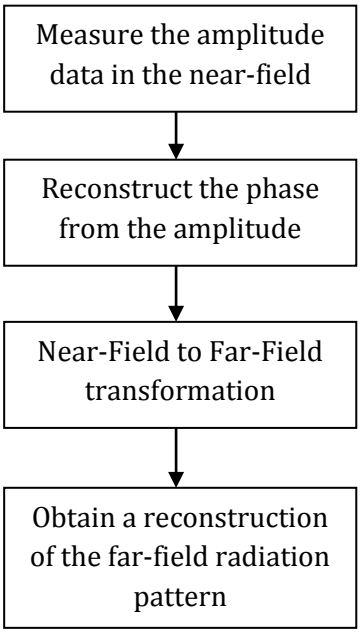

Figure 3: General procedure to reconstruct the Far-Field from near-field amplitude only measurements.

The amplitude measurements are going to be taken over two planar surfaces located few wavelengths away from the antenna aperture. Then, by applying the iterative Fourier algorithm, the phase will be reconstructed from the amplitude measurements. This method is going to be introduced in Chapter 3.

In the following Chapter, the main principles of the planar-near field are introduced. The transformation to compute the far-field radiation pattern from the near-field measurements is also briefly addressed in Chapter 2.

2 Planar Near-Field Antenna Measurements

2.1 Near-field antenna measurements

The near-field antenna measurements have gained fame during the last years because since it avoids some of the drawbacks of the far-field antenna measurements. Such techniques are usually performed indoor, and they offer a high grade of accuracy. Apart from that, they are cost and time effective.

The measurements in the near-field have to be taken over some preselected surface such as planar, cylindrical or spherical surfaces [2]. Obviously, there are too many different surfaces that we can use to carry out the measurements but the computational complexity of obtaining the far-field radiation pattern will depend on the surface selected. Actually, the complexity of the measurement system is increased from the planar to the spherical. The choice of the correct surface is based on the antenna to be measured. In this thesis the planar technique will be used due characterize a moderate gain Horn antenna.

The procedure to achieve the far-field pattern of the antenna from the near-field measurements is quite easy to understand. First of all, we take the measurements over the preselected surface with a scanning probe or another radiating device. The location of the preselected surface has to be close to the antenna, but out of the reactive near-field region. In other words, we usually locate the surface some wavelength away from the antenna under test. Once we achieve the measurements in near-field some Fourier techniques that we are going to explain a bit later can be employed to compute with a high level of accuracy the far-field pattern [2].

In the following Figure, the different generic architectures usually employed in neat-field antenna measurements are represented:

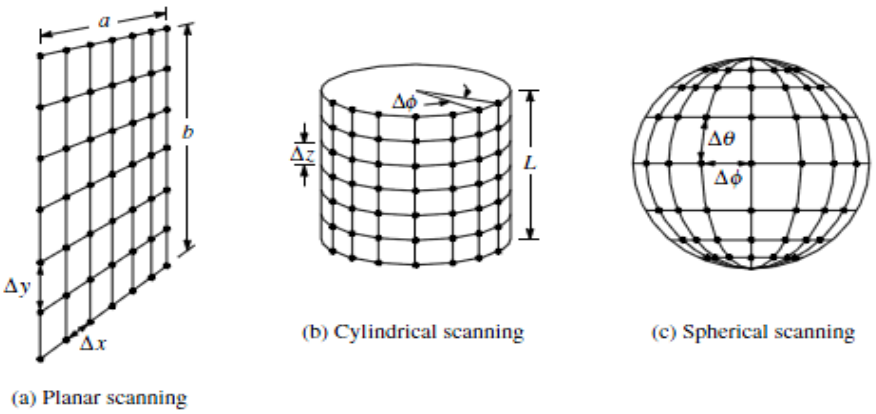

Figure 4: Standard scanning surfaces used in near-field antenna measurements [Principles of Planar Near-Field Antenna Measurements, Stuart Gregson, John McCornick and Clive Parini]

2.1.1. The planar architecture

We will choose a rectangular coordinate system so that the antenna aperture lies in the plane z=0. The plane over which the measurements must be taken is located few wavelengths from the antenna aperture as it shown in Figure 5, so that we are out of the reactive near-field region.

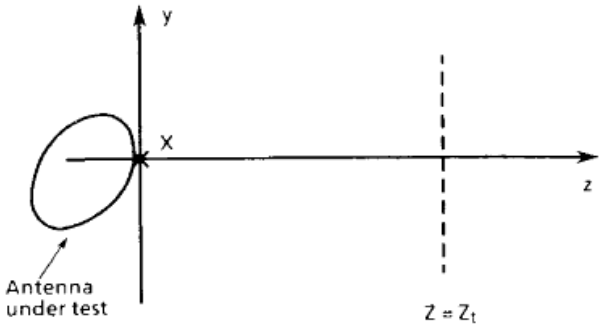

Figure 5: Geometry of planar near-field measurement [An examination of the theory and practices of Planar Near-Field Measurements, Johnson J.H. Wang]

The planar measurement configuration can be subdivided into three different categories: plane bipolar, plane polar and the most commonly used, plane rectilinear [2]. All of these different configurations can be appreciated in Figure 6:

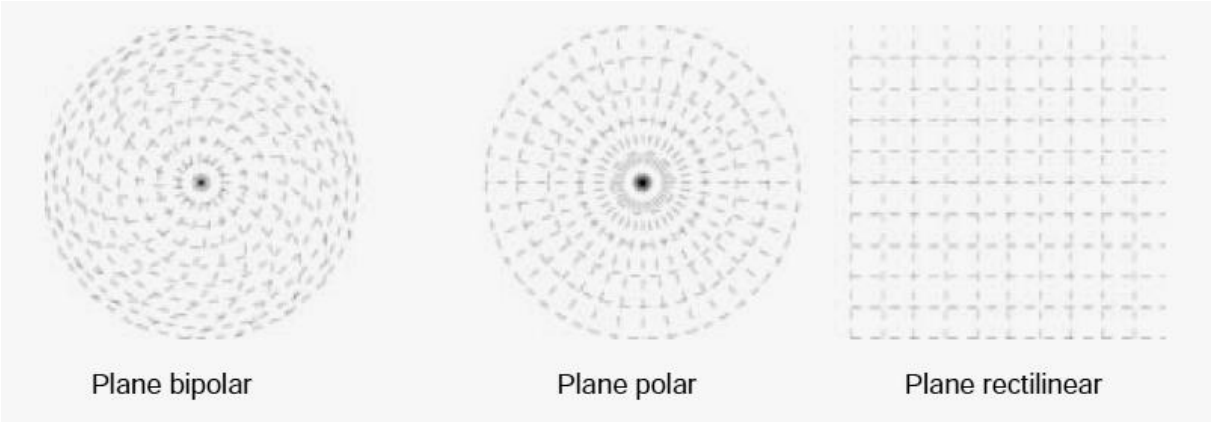

Figure 6: Different configuration for the planar measurement system [Principles of planar near-field antenna measurements, Stuart Gregson, Jon McCorcnick and Clive Parini, Figure 3.10].

For the development of this thesis, the third configuration has been selected, so that the near-field measurements are taken over a rectilinear planar surface. In Figure 7, the general configuration for planar near-field measurements by using rectilinear planes is shown:

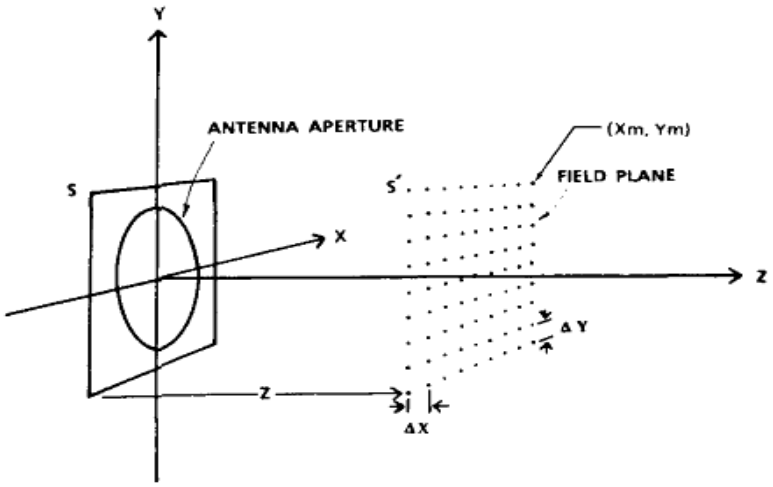

Figure 7: Architecture of the rectilinear scanning plane. [An examination of the theory and practices of Planar Near-Field Measurements, Johnson J.H. Wang]

The maximum sample spacing between two sample points in vertical and horizontal directions are determined by the following expression:

$$\Delta x = \Delta y = \lambda/2 \tag{2.1}$$

The plane over which the measurements will be made is divided into a rectangular grid of MxN points with a maximum spacing of $\lambda/2$ in order to satisfy the Nyquist sampling criterion.

2.2 The Near-Field to Far-Field transformation

Once we have the measurements in the near-field, and a complete characterization has been obtained, we can compute the far-field radiation pattern by applying a mathematical transformation. The mathematical procedure is basically based on a simple Fourier transformation.

Depending on the surface over which the near-field measurements have been taken, we can construct a planar, cylindrical or spherical near-field spectrum. This spectrum is basically the representation in the frequency domain of the near-field antenna distribution. In our case, we are going to be focused on the planar architecture, so that the near-field measurements are taken over a plane grid (or two scanning planes, as we will see in Chapter 3) located in the radiating near-field region, so that from these measurements the planar wave spectrum (PWS) can be constructed over the planar surface.

There is a direct relationship between this spectrum and the field radiated in the far-field region: an inverse Fourier transformation:

$$\underline{E}(x=ru, y=rv, z=rw) = \frac{1}{4\pi^2}\int_{-\infty}^{\infty}\int_{-\infty}^{\infty}\left[\underline{F_T}(k_x, k_y, z=0) - \hat{e}_{\underline{z}}\frac{\underline{k_T}\cdot\underline{F_T}(k_x, k_y, z=0)}{k_z}\right]\times e^{-jr(k_x u+k_y v+k_z w)}\,dk_x dk_y \tag{2.2}$$

In the previous expression, F_T are the orthogonal components of the plane wave spectrum over the scanning plane, which are expressed in terms of k_x and k_y , the orthogonal wavenumbers of the spectrum. In that expression, E is basically the electric field elsewhere, so that in order to compute the far-field radiation pattern from the plane wave spectrum we only have to evaluate the previous equation at a infinite distance away from the antenna.

Since the electric near-field measurements are taken over a scanning surface, the reconstruction of the spectrum is made from sample points of the tangential electric components. The spectral wavenumbers where the PWS is going to be described are as follows:

$$k_x = \frac{2\pi m}{M\Delta x}, \qquad -\frac{M}{2} \le m \le \frac{M}{2} - 1 \tag{2.3}$$

$$k_y = \frac{2\pi n}{N\Delta y}, \qquad -\frac{N}{2} \le n \le \frac{N}{2} - 1 \tag{2.4}$$

Where M and N are the number of sample points over the scanning plane in the x and y directions and Δx and Δy are the sample spacing between two sample points. By evaluating the equation (2.2) at a long distance away from the antenna, we can obtain the radiation far-field pattern from the planar near-field spectrum. Nevertheless, for the majority of the antennas, the evaluation of this expression is too complicated and a suitable approximation is needed. Such approximation comes from the principle of the Stationary Phase and allows us to use another useful expression to compute the far-field from the planar near-field expression:

$$\underline{E}(ru, rv, rw) \approx j\frac{e^{-jkr}}{\lambda r}\cos\theta\,\underline{F}(k_x, k_y) \tag{2.5}$$

Therefore, the procedure to compute the far-field radiation pattern from the near-field measurements (with both, amplitude and phase) is described in the following figure:

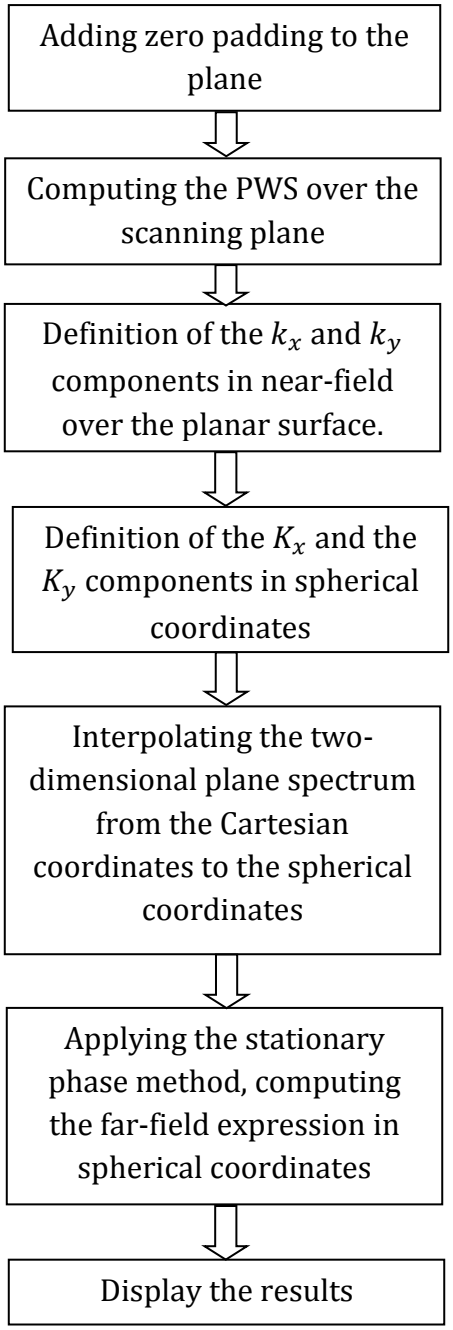

Figure 8: Flow-Chart of the NF-FF transformation.

First of all, it is highly convenient to add virtual sample points to the plane (those points are set to zero) in order to enhance the far-field prediction accuracy. Theoretically, reducing the sample spacing between sample points does not enhance the resolution of the estimation, providing that the sample spacing satisfies the Nyquist criterion, obviously. Nonetheless, increasing virtually with zero padding the samples will help significantly the resolution of the transformation. The explanation is because by adding virtual points set to zero values, we are taking more points to sample the plane wave spectrum of the near-field, and this results in improving the accuracy of the reconstructed far-field radiation pattern.

In the following Figures, Figure 9 and Figure 10, the reconstruction of a far-field radiation pattern in H-Plane and E-Plane is shown. The antenna used is a horn antenna working at 12 GHz, and the plane is located at 3λ.

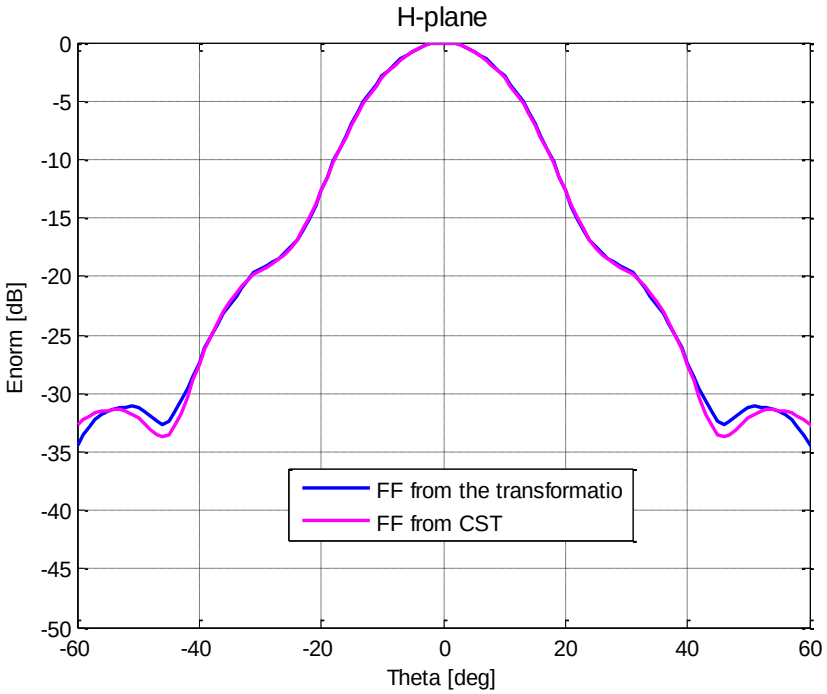

Figure 9: Reconstruction of the FF in H-Plane

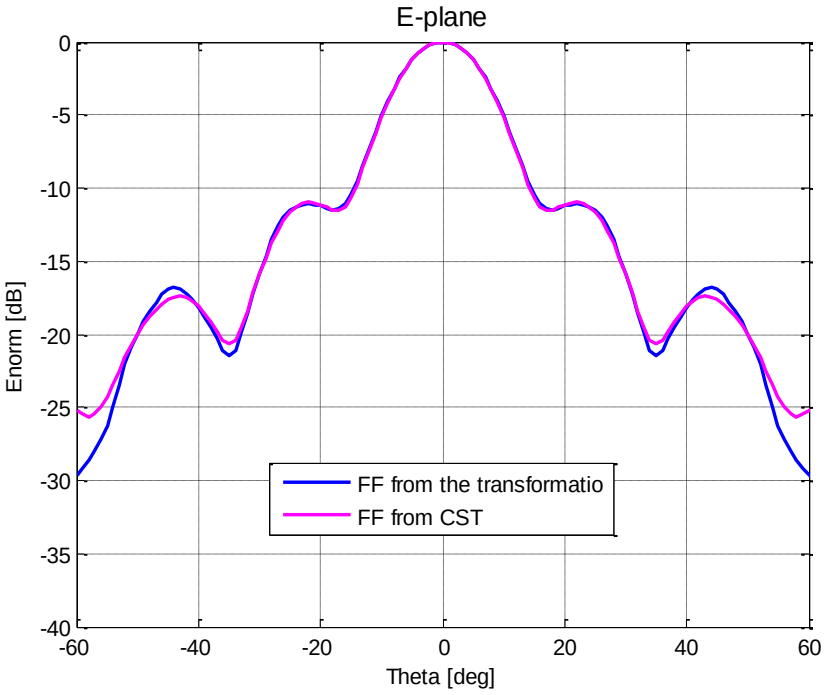

Figure 10: Reconstruction of the FF in E-Plane

The transformation works really well for the central part of the cut but is worse in the extremes of the graph. This is due to the finite dimensions of the plane that produce the truncation effect. The equation (2.6) gives us an approximation of the valid far-field range that can be expected.

$$valid\ angle\ (rad) = \text{atan}(\frac{xWidth-D-P}{2z}) \quad (2.6)$$

In the above expression, xWidth is the dimension of the plane; D is the dimension of the antenna aperture and P the dimension of the probe we are using. On the other hand, z is the distance away from the antenna aperture where the plane is located. In Figure 11, a graphical representation of all of those parameters is shown:

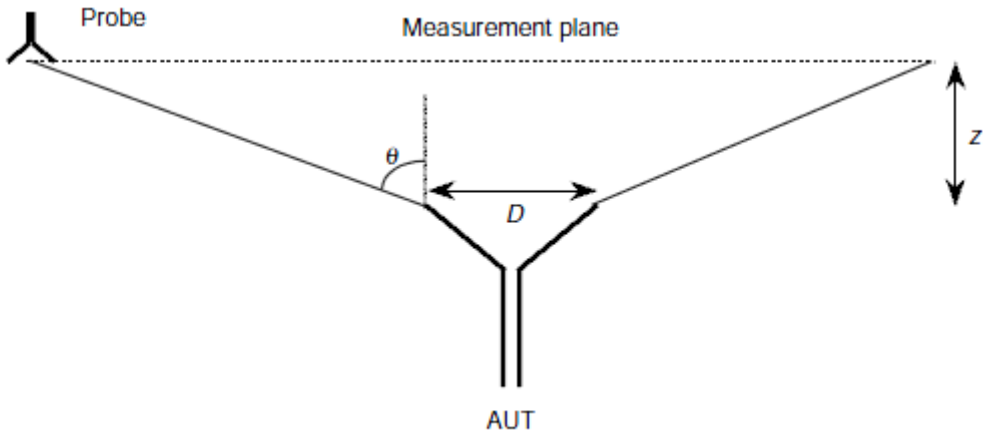

Figure 11: The valid angle of the planar near-field antenna measurements [Principles of planar near-field antenna measurements, Stuart Gregson, Jon McCorcnick and Clive Parini, Figure 5.2]

3 The Phase Retrieval Method

3.1 Introduction

In the previous chapter, the transformation used to compute the far-field radiation pattern of the antenna from the near-field measurements has been shortly explained. As it was pointed out in the introduction, we need both, the amplitude and the phase. In this case, as we said, we have to reconstruct the phase information from the amplitude measurements.

The idea of the phase reconstruction from only amplitude data is not completely new. Other scientific areas have tried to set forth that procedure, such as in optics or electron microscopy. In the antennas domain, the concept came out in the 1980s and the first works in near-field measurements based on amplitude data were published in 1990s by Naples group of scientists. During the 1990s the scientist from the University of California, (UCLA) started to solve the problem of phase reconstruction as well.

There are two different configurations that we can use to take the amplitude data:

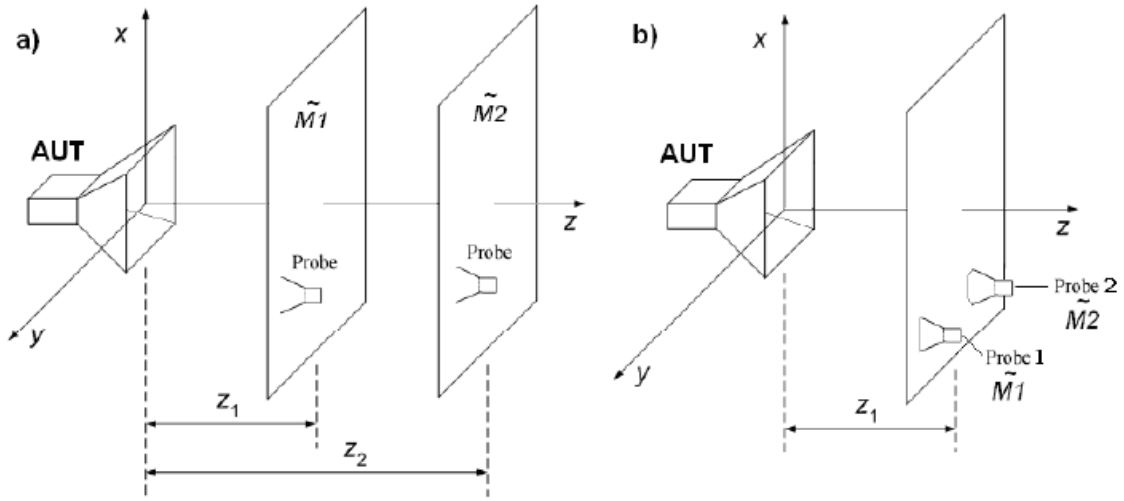

Figure 12: Planar Near-Field Antenna Measurements architecture to take amplitude data [Reconstruction of the Near-Field, Doctoral Thesis, Jan Puskely, Figure 2.1]

The first option consists of two scanning planes located at the radiating near-field zone and separated a few wavelengths from the antenna aperture. The separation between the planes is an important factor to take into account during the reconstruction of the phase, and ideally they should be separated as much as possible so that the amplitude data taken over the planes can be more different, since this difference helps in the procedure of the reconstruction. For example a separation of two or three wavelengths is appropriated.

The second option consists of a single scanning plane where the amplitude data are taken by using two different scanning probes. Since those probes are going to measure the amplitude

over the same surface, their radiation patterns have to be different. During the development of this project, the first architecture was chosen.

First of all, an introduction to the different phase retrieval methods will be explained in this chapter. The different branches of algorithms used to reconstruct the phase from the amplitude information, such as iterative algorithms or functional minimization methods are going to be explained.

3.2 Current phase retrieval methods

Currently, there are different approaches to find the phase distribution from the amplitude, and they have a huge application in the near-field antenna measurements problematic. Different techniques have been developed, but we are going to concentrate on those techniques based on the minimization of a cost function.

3.2.1 The functional minimization methods

The functional minimization methods are based on the minimization of a cost function. The goal of those methods is to find the complex near-field distribution that minimizes a defined cost function. That cost function is going to be basically the difference between the calculated amplitudes in each step of the method and the amplitude measurements taken over the two scanning planes.

The algorithms we are talking about can be divided into two groups: local and global methods [4]. In the following figure (Figure 13), a brief description of those types of algorithms is going to be introduced.

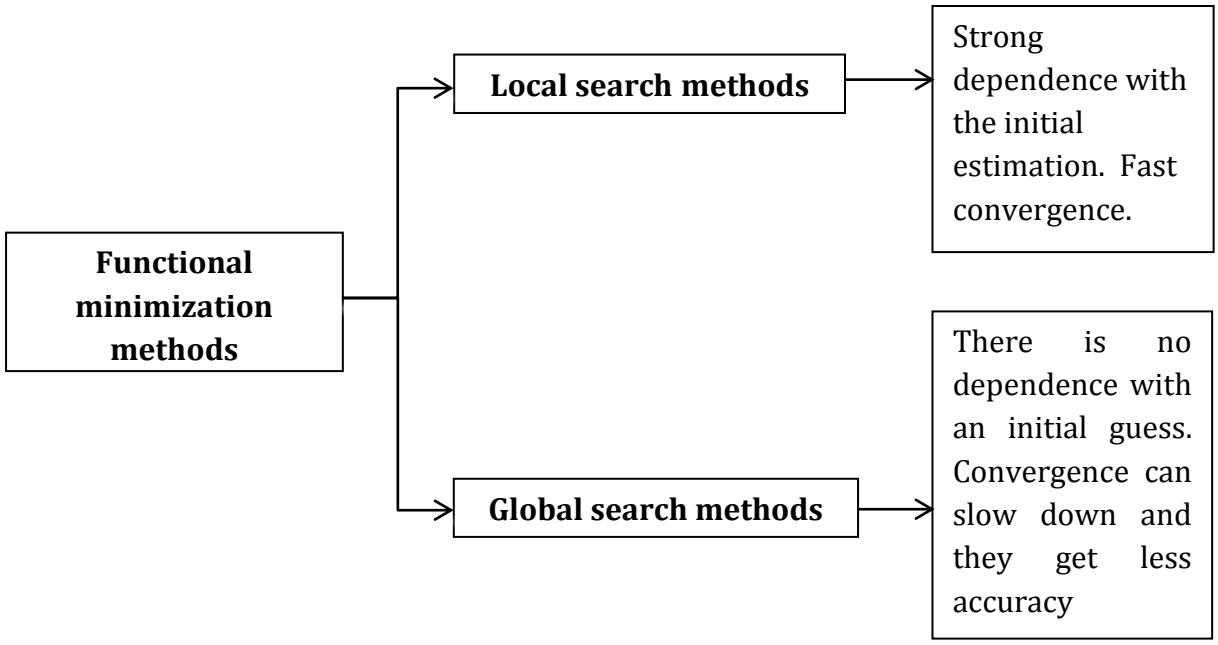

Figure 13: Classification of the Functional Minimization Methods.

The local minimization is used when choosing an initial estimate in the area of the global minimum. The goal is to find the minimum value of the functional. The field distribution with which we find the minimum value of the cost function is the most suitable estimation of the near-field, so that this is a good procedure to reconstruct an estimation of the phase. Consequently, several efforts have to be paid to find the global minimum of the cost function. The local search is more straightforward and faster than the global optimization procedures, providing that the initial guess of the near-field distribution rests close to the global minimum. Therefore, in spite of the fact that local searches are easier, there is a strong dependence on the initial guess of the near-field [4].

One of the traditional local optimization procedures is the well-known as hill-climbing algorithm [19]. With the aim to demonstrate that a local search is not an optimal choice when the cost function is complex and has various local minima, an example of hill climbing algorithm has been programmed in order to minimize a complex cost function. The selected cost function presents various local minima and just one single global minimum. This cost function is described by the following expressions:

$$cost = f(x,y) = xsin(4x) + 1.1ysin(2y) \quad (3.1)$$

$$0 \leq x \leq 10\,, \quad 0 \leq y \leq 10 \quad (3.2), (3.3)$$

The surface of this cost function is represented in the following Figure:

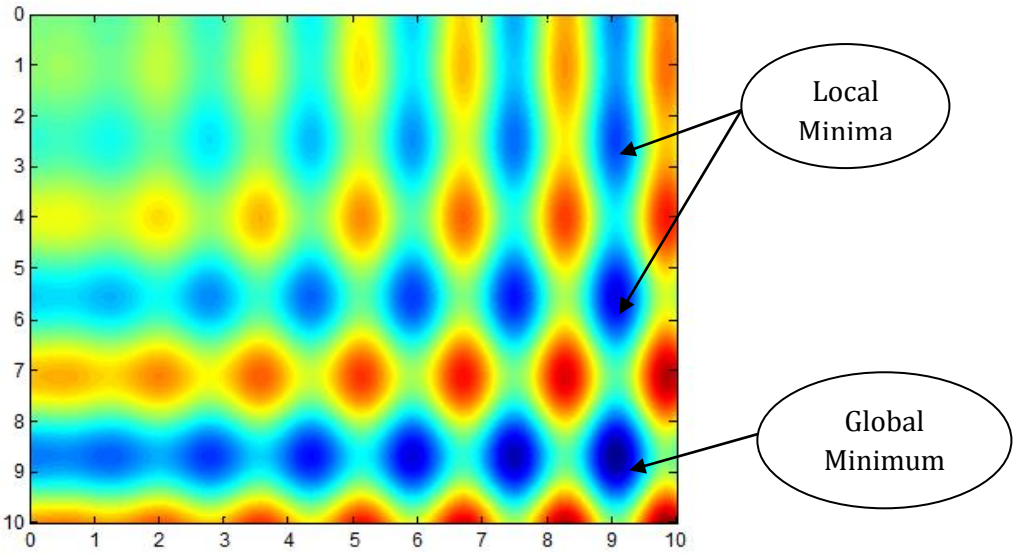

Figure 14: Cost function surface

Hill-Climbing is optimal to find a local minimum (or maximum) of the cost function in the search domain, which is specified by the initial variables of the algorithm. Nevertheless, if

those initial points define a search domain where the global minimum is not located, the local search will probably fail in finding the optimal solution.

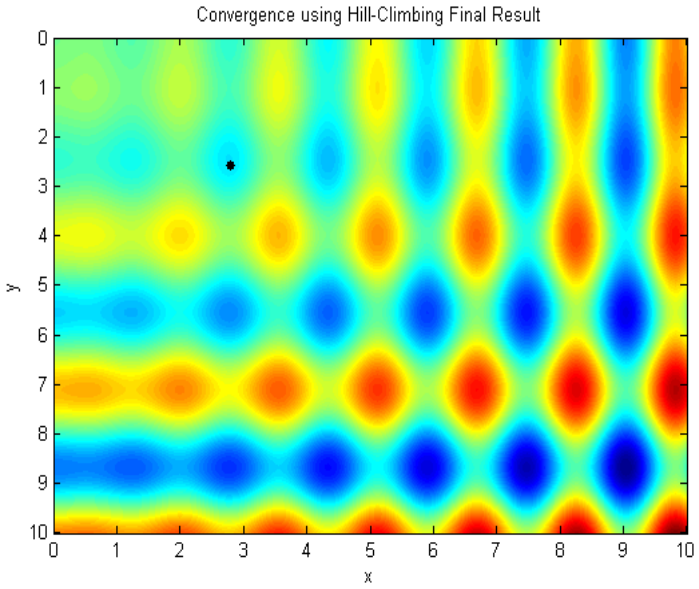

Figure 15: Hill-Climbing with search domain between 0 and 4

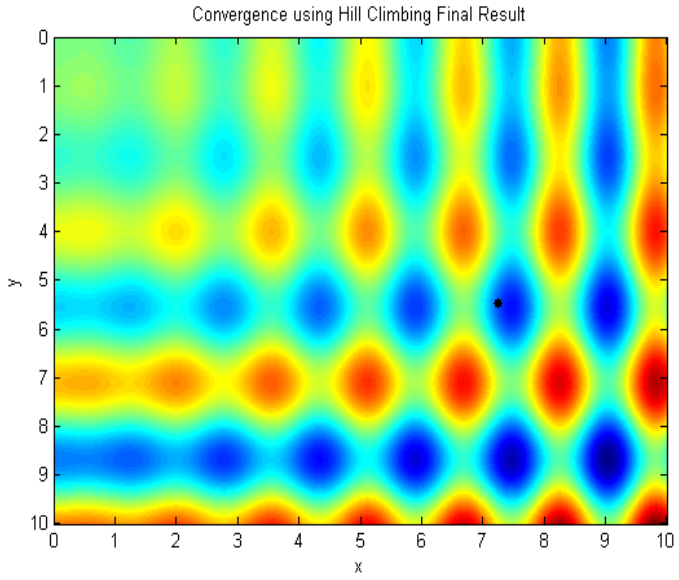

Figure 16: Hill-Climbing with search domain between 0 and 8

In contrast with the local search, the global search does not rely upon the initial estimation because it produces an intensive search over different valleys of the selected functional. Nevertheless, the convergence can slow down. Apart of that, global procedures are less straightforward and more complicate to program. Global searches cannot get a huge accuracy; hence, a combination of the global methods and the local ones is usually looked for.

3.2.2 Fourier Iterative Algorithm

The Fourier Iterative Algorithm (FIA) works as follows:

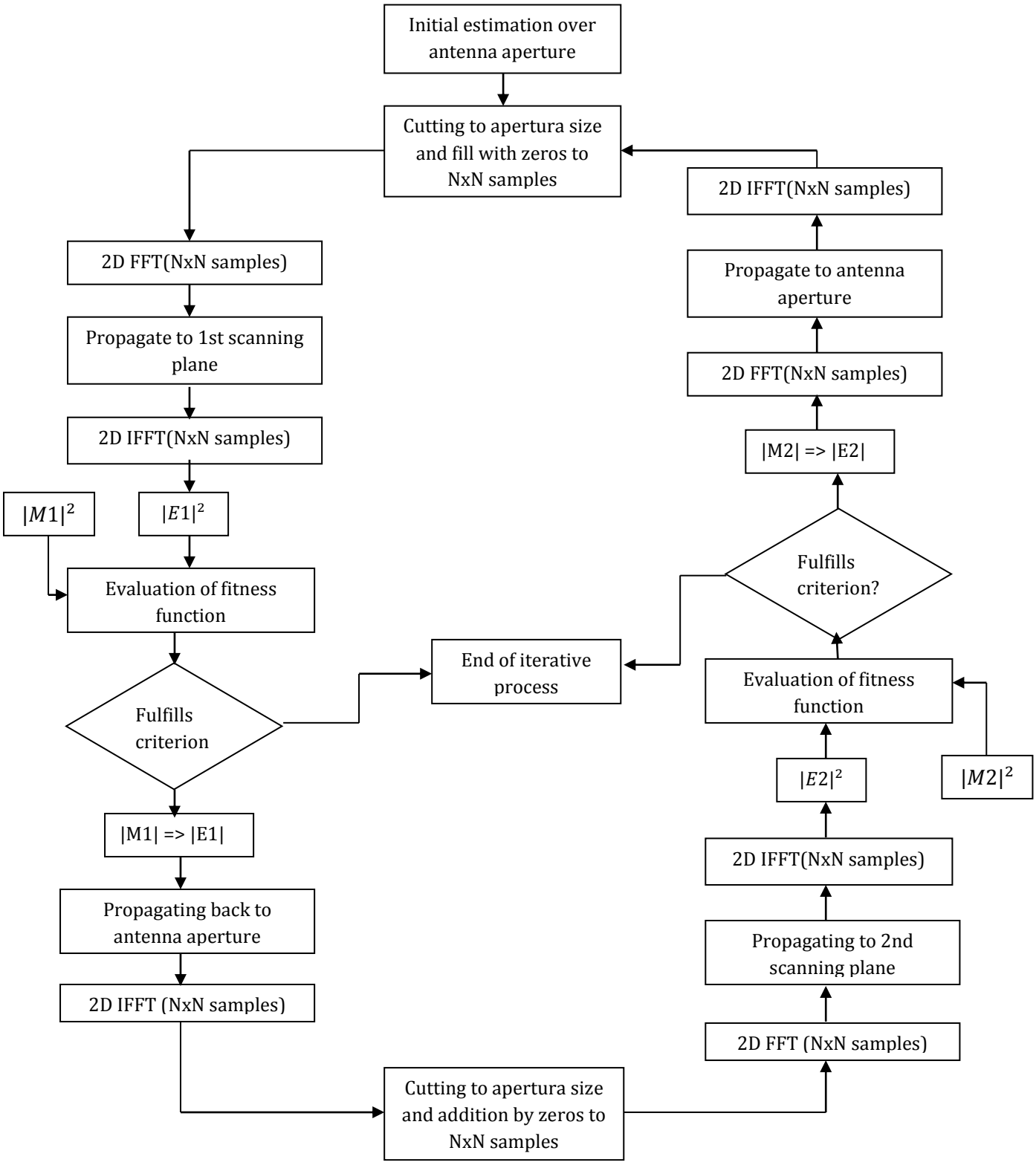

Figure 17: Flow Char of the classical Fourier Iterative Algorithm.

The procedure is simple. Firstly, an initial guess of the complex field over the antenna aperture needs to be established. Then, the initial guess is filled with zeros until the dimensions of the scanning plane. The plane wave spectrum over the antenna aperture is calculated and propagated forward the first scanning plane. There, the field is obtained again from the spectral domain and the cost function is evaluated. Whether the minimum cost function has been reached, the algorithm stops. Otherwise, the calculated amplitudes are replaced with the measured ones and the field is propagated back to the antenna aperture where the constraint is applied (basically, the propagated field has to be truncated again to the aperture dimensions). The same procedure is repeated again with the case of the second scanning surface, and the algorithm is repeated until the difference between the calculated amplitudes and the measurements is lower than a certain value in one of the two planes or a maximum number of iterations has been reached.

The Fourier Iterative Algorithm has been widely used to reconstruct the phase distribution from the amplitude data in the near-field antenna measurements, and is pretty appropriate for the architecture with two scanning planes. Nonetheless, due to the strong dependence with the initial estimation, for some particular antennas if the initial estimation is too rough the algorithm can stagnate. Therefore, our goal is to find a suitable initial guess of the field over the antenna aperture so that the algorithm does not stagnate. The search of this initial estimation of the field is going to be developed by a global optimization method.

3.3 The Global Optimization

3.3.1 Overview of the Global Optimization Procedure

The method selected to find this initial estimation of the field is based on a global optimization search, as it was pointed out above. Once again, the goal is to minimize a selected cost function, which is once again the difference between the calculated amplitudes and the measured ones over the scanning planes. Since no previous knowledge is had about the near-field phase distribution, we need an algorithm that approaches us to the region of the global minimum of the functional.

Two different approaches have been used to implement the global optimization procedure. The first one implements separately the Global Optimization and the Fourier Iterative so that Global Optimization tries to find the initial estimation of the field as a support technique to FIA. In the second approach, which is still based on the minimization of a cost function in order to retrieve the phase from amplitude data, the Global Optimization and the Fourier Iterative Algorithm are combined in the same algorithm so that we obtain a better estimation of the near-field phase, as we will see in the simulations shown in Chapter 5. Both methods are going to be explained in the following epigraphs.

3.3.2 First method for the Phase Retrieval Problem

The first method implements separately the GO and FIA. In the following figure, Figure 18, a description of the procedure to reconstruct the phase is briefly included:

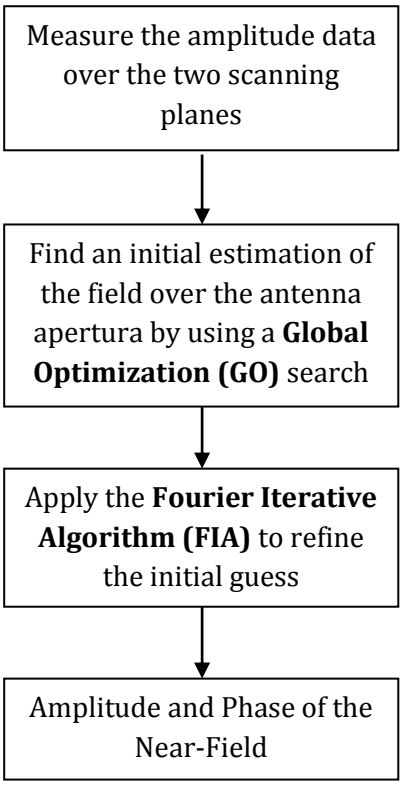

Figure 18: Procedure to reconstruct the phase from only amplitude data in the near-field.

With the Global Optimization, we are going to optimize a set of variables. Those variables are the complex sample points over the antenna aperture whose suitable distribution is looked for. The optimization of those points is going to be oriented by the minimization of the cost function, as we explained previously, so that the appropriate field over the antenna aperture should minimize the difference between the calculated amplitudes and the measurements over the scanning planes. The number of variables that are going to be optimized over the antenna depends on the sample spacing chosen and, of course, on the dimensions of the antenna.

In the following figure, a flow char of the procedure to find this initial guess of the complex field over the antenna is shown:

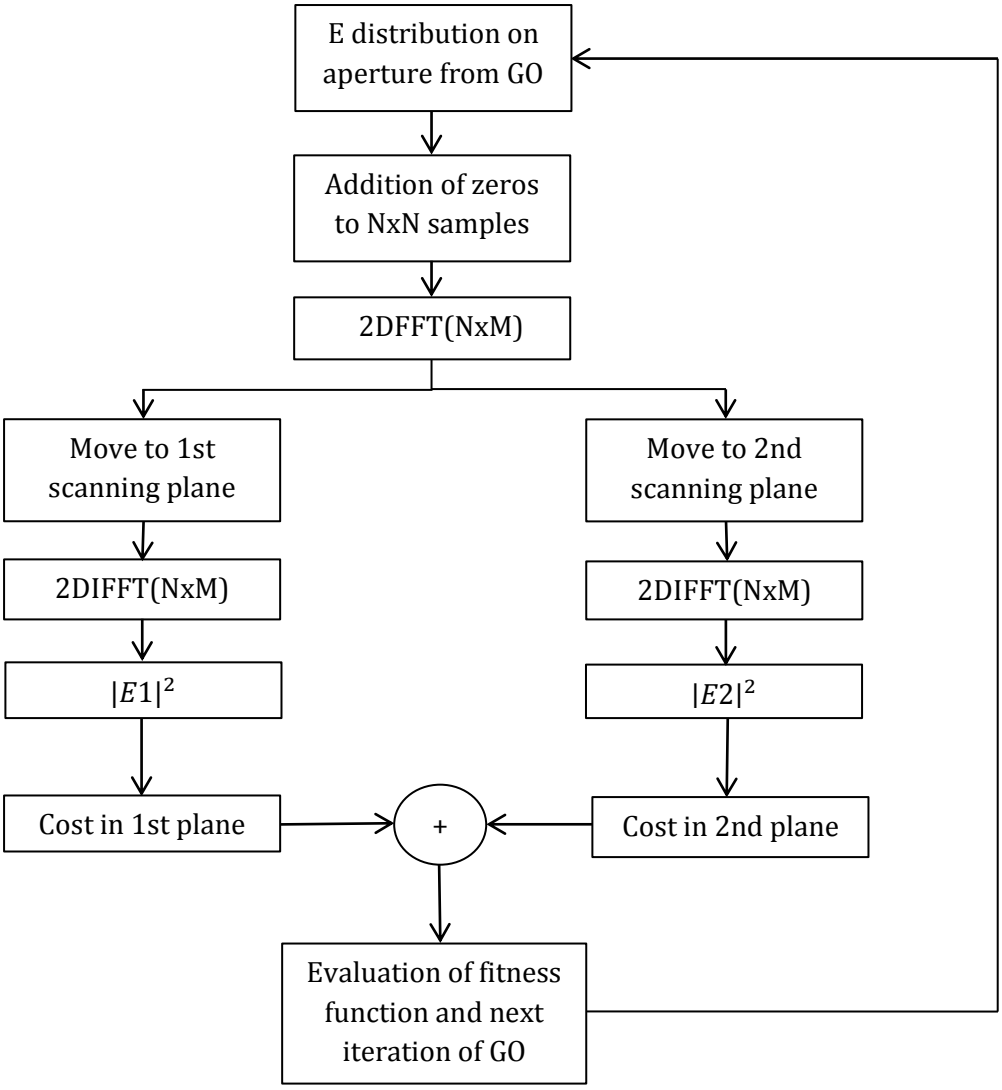

Figure 19: Flow Char of the first version of Global Optimization.

The algorithm starts with an initial and random estimation of the field over the antenna aperture. Then, this initial estimation is filled with zeros to the dimensions of the scanning planes, NxM. Successively, the algorithm branches into two different arms, and each arm will study the behavior of the field over the antenna aperture with the cost function in each scanning plane. The planar wave spectrum of the estimation over the antenna aperture is calculated by applying a FFT algorithm and propagated forward each scanning plane. There, the cost function is evaluated (as it was said, the difference between the calculated amplitudes of the field and the amplitude measurements in each scanning plane) and the stop criteria is checked. The stop criterion can be either, whether the minimum value of the cost function has been reached or a maximum number of iterations have been made. Whether the stop criterion

is not accomplished, a new iteration of the Global Optimization is made, and again the estimation of the field over the antenna aperture is optimized, otherwise, the algorithm stops and the field distribution over the antenna aperture becomes the initial guess that has to feed the Iterative Fourier Algorithm. In the following Figure, the previous algorithm is explained by using a draw of the physical architecture that we are using:

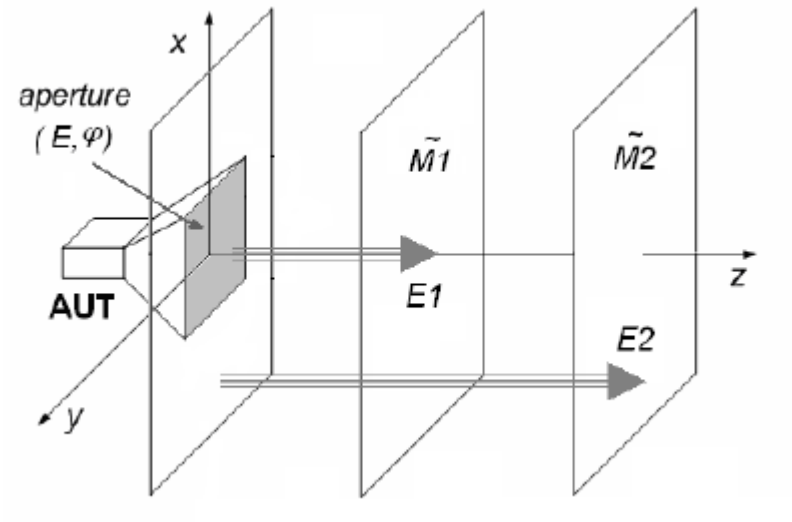

Figure 20: Schematic representation of the first version of the Global Optimization procedure [Reconstruction of the antenna near-field, Jan Puskely, Figure 3.17]

3.3.3 Second method for the Phase Retrieval Problem

In this second version, the Global Optimization and the Fourier Iterative Algorithm are implemented in the same method, not separately. The principle is the same: we are looking for an estimation of the near-field by minimizing a cost function, which is the difference between the calculated amplitudes and the measured ones over two scanning planes. However, in this case, the Global Optimization and FIA are combined. The Genetic Algorithm works to find a estimation of the field over the antenna aperture and in each iteration, the Fourier Iterative Algorithm is applied so that this estimation of the field over the antenna aperture is enhanced.

With this technique, the cost function is evaluated on the first scanning plane. If the stop criterion is not accomplished, the field after the replacement of the calculated amplitudes with the measurements is propagated back to the antenna aperture, where the Global Optimization will work again generating a new estimation of the field over the aperture.

A really similar algorithm was used in [4] to find the initial guess of the field over the aperture obtaining better results.

In Figure 21, a flow char of this last procedure is shown. Moreover, in Figure 22 we represent the algorithm in terms of the physical architecture that we are using, as we did in Figure 20.

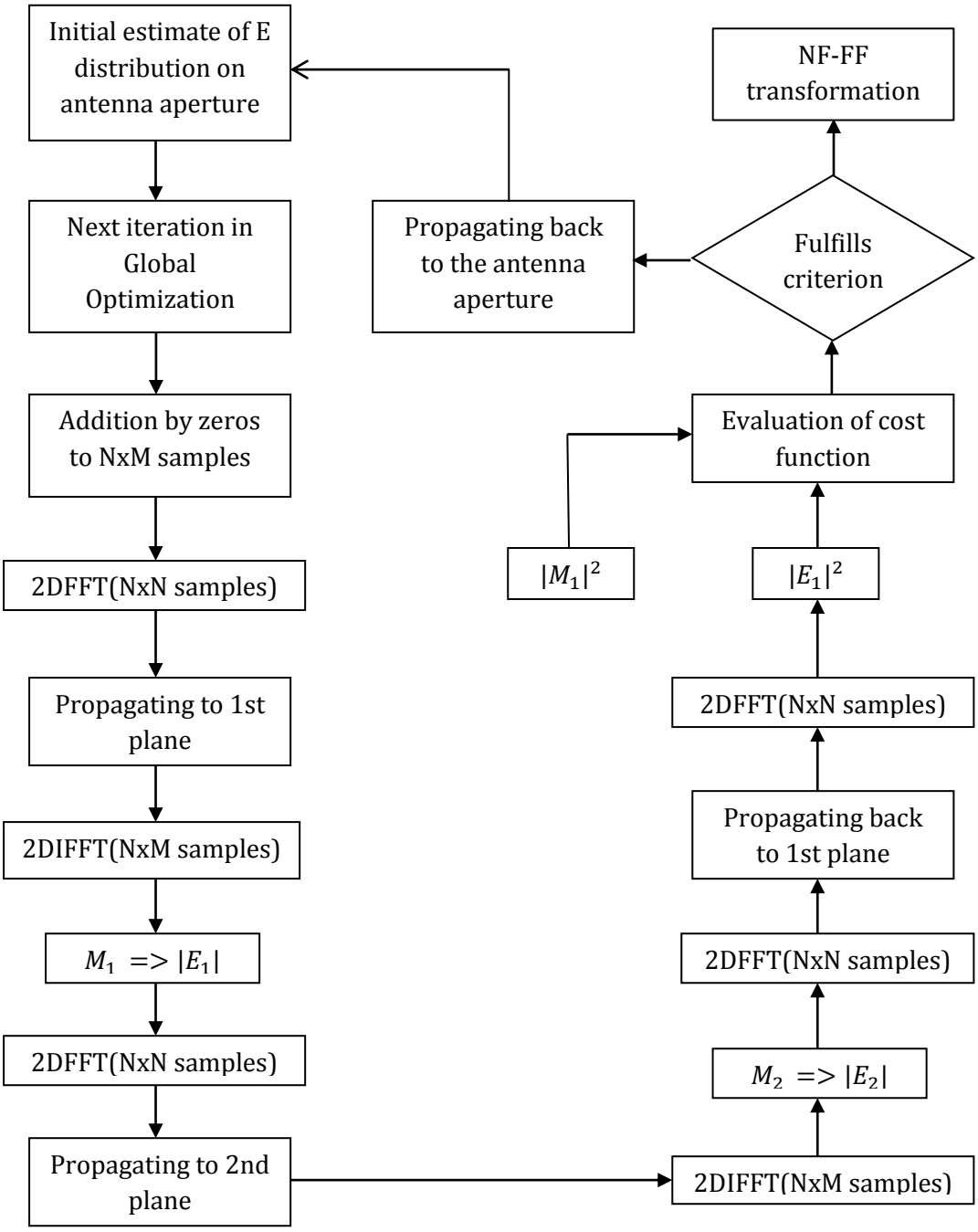

Figure 21: Global Optimization based on the principle of Fourier Iterative Algorithm

Figure 22 was extracted from [4] in order to explain the procedure of the algorithm graphically. In this figure, the new contribution to this algorithm has been added.

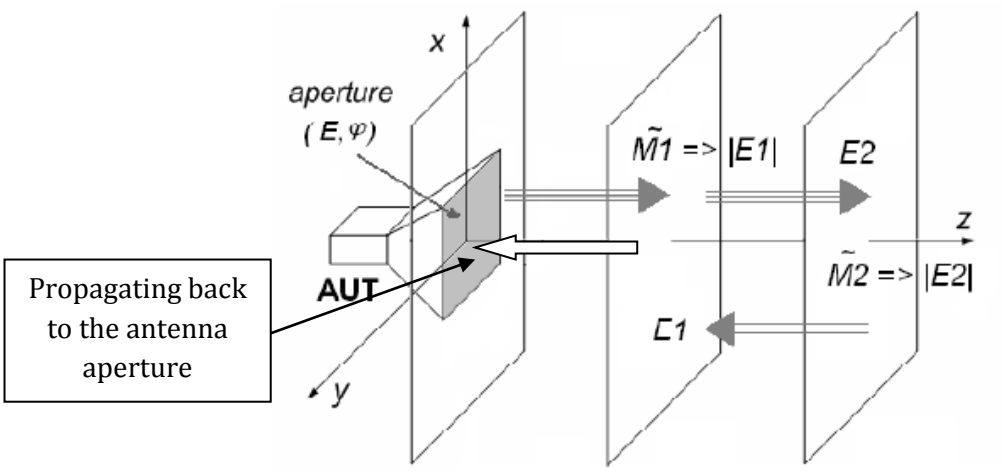

Figure 22: Schematic representation of the second version of GO

Now, it is time to explain the possible methods that we can use to optimize in each iteration of the previous algorithms the complex field of the antenna aperture.

3.3.4 Natural Optimization Algorithms

We can use deterministic techniques and stochastic techniques as global methods to find the suitable initial guess of the field. Since no previous knowledge of the phase is known, the initial variables must be randomly generated, and the stochastic procedure is more appropriate.

The Natural Optimization Algorithms are methods that we can use for this purpose, and they optimize variables by applying operators based on natural procedures [3]. Some of them are Simulated Annealing (SA), Particle Swarm Optimization (PSO), Differential Evolutionary Algorithms (DEA) or Genetic Algorithms (GA).

The Genetic Algorithm has been the Global Optimization algorithm chosen for the development of this thesis. A suitable explanation of the most important characteristics of Genetic Algorithms are explained in the following Chapter, and the characteristics of the Genetic Algorithm used to achieve the initial estimation of the field over the antenna aperture are also addressed in Chapter 4.

3.4 On the uniqueness of the phase from amplitude-only data.

3.4.1 Overview of the problem.

In this chapter, algorithms to reconstruct the phase from the amplitude data in the near-field region of an antenna have been explained. The Fourier Iterative Algorithm was introduced as a straightforward of retrieving the phase from the amplitude data over two scanning planes. Nevertheless, this algorithm depends on the initial estimation of the field, so in some circumstances the algorithm can stagnates whether the initial condition is not appropriated. In order to solve this, a Global Optimization procedure is developed to find the initial estimation of the field over the antenna aperture and, with this initial estimation we feed FIA to refine the phase of the near-field.

However, we have to face with other problem: the fact that for one particular amplitude distribution there exist several possible phase distributions. That means that the phase is not unique. This fact can be explained from the following theorem:

Theorem: *Let* $x[n]$ *and* $y[n]$ *be two sequences whose z-transform contain no-reciprocal pole-zero pairs and which have all-poles, not at* $z = \infty$*, inside the unit circle, and all zeros, not at* $z = 0$*, outside the unit circle. If the magnitudes of the Fourier transform of* $x[n]$ *and* $y[n]$ *are equal, then* $x[n] = \pm y[n+m]$ *for some integer* m*.*

The theorem is explained for one-dimensional sequences, but their properties can be easily extended to two-dimensional sequences, for example, our set of measurements over the scanning planes.

Of course, if we have $x[n]$ and $y[n]$, two sequences, we can define the z-transform of both of them, so that:

$$x[n] \rightarrow X(z)$$

$$y[n] \rightarrow Y(z)$$

Both sequences are defined over the unit circle in the z-domain; so that the Fourier transforms can be defined (the Fourier transform converges over the unit circle). And the magnitudes of the Fourier transforms are equal:

$$|X(z)| = |Y(z)|$$

$$|X(j\omega)| = |Y(j\omega)|$$

We can define G(z) = X(z)/Y(z). Since X (z) and Y(z) have the same magnitude on the unit circle, G(z) must be entirely all-pass with unit magnitude, so that if X(z) has a zero at $z = z_0$, necessarily Y(z) must have a pole at $z = 1/z_0^*$ and vice versa.

Therefore, G(z) must be of the form:

$$G(z) = \pm z^m$$

And that means that $x[n] = \pm y[n+m]$.

With this principle, we obtain that for one sequence whose Fourier magnitude is known we can obtain multiple phases, because multiple different sequences can have that similar phase. Translated to our problem, we can reconstruct one of the possible phases for the particular amplitude measurements in the near-field, but we cannot guarantee this phase is unique.

This problem is a typical problem in the reconstruction of images using iterative techniques, such as the Fourier Iterative Algorithm. This is the problem of simultaneous twin images which has been reported widely in the literature [21]. The algorithm tries to reconstruct an image, but this image has a twin with the same Fourier modulus (for example Figure 23 (a) and Figure 23(b)). If the algorithm starts with a random initial guess, both images have the same probability of being reconstructed. The problem arises when during the first stages of the algorithm, features of both objects are reconstructed simultaneously. Then, the algorithm can stagnate. This is the example of Figure 23(c).

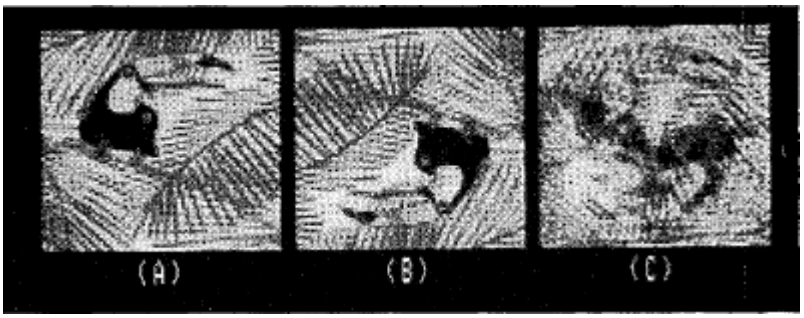

Figure 23: Example of the simultaneous twin-images problem [Phase-retrieval stagnation problems and solutions, J.R.Fienup and C.C.Wackerman].

In the case of the reconstruction of the near-field phase from the near-field amplitude occurs the same. For instance, the Fourier Iterative Algorithm can stagnate because there are two possible phase distributions for the same amplitude distributions and both are equally strong. We should take care especially during the first stages of the algorithm.

During the development of this project, two solutions are raised: the first one is to give priority to one of the possible phases during the first stages of the algorithm. The other one is to use the global optimization technique to achieve an initial estimation of the phase over the antenna aperture, so that the Fourier Iterative Algorithm starts from this initial guess giving priority to one of the possible phases.

3.4.2 Some theoretical solutions to the problem.

As it was mentioned, two solutions are raised during the development of this thesis:

1. **The reduced-area support constraint method.**

The reduced-area support constraint method is really appropriated for the iterative technique in the reconstruction of the phase from the amplitude data. Basically, it consists of using a reduced-area support as the pattern of the antenna aperture during the first iterations of the algorithm. Then, when a number of iterations has been made (for example, 10 or 20 iterations) the reduced area is replaced with the total area support constraint, so that an initial estimation of the phase over the antenna aperture can be obtained.

By acting like this, the reduced-area support constraint tends to favor some of the features and then, when the correct support is established again, one of the features has advantage respect the other one. In the following figure, Figure 24, both types of supports, the partial and the total one are shown:

Figure 24: Reduced-area support constraint and total area constraint for the antenna aperture

2. **The estimation of a suitable initial guess over the antenna aperture.**

In this case, the search of a suitable initial guess of the field over the antenna aperture can help us with this problem. By using the Global Optimization, which is based on a Genetic Algorithm, we create a rough initial estimation of the complex field over the antenna aperture. In other words, we find an initial estimation of the phase, and with this initial guess we feed the FIA. In this case, with this initial guess, we are orienting the iterative algorithm to reconstruct a particular solution of the phase. As we will be able to check on the results shown in Chapter 5, when the Global Optimization is performed and an initial guess of the phase over the aperture is found, the final reconstructed phase always follows the same pattern that the initial estimation.

4 The Genetic Algorithm

4.1 An Overview of Genetic Algorithms

4.1.1 Introduction to Genetic Algorithms

The Genetic Algorithm has been chosen as the global method to optimize the field over the antenna aperture so that we can find the initial guess of this field. In this section, 4.1, we are going to present an overview of the Genetic Algorithms. Then, in section 4.2, we will see how to apply the Genetic Algorithm to the problem of phase retrieval.

The Genetic Algorithm is an optimization and search technique based on the principles of genetics and natural selection [3]. The Genetic Algorithm allows a population formed by individuals to evolve creating different generations of individuals that try to minimize or maximize a selected cost function. The evolution of the generations of individuals is governed by genetic operators such as natural selection, crossover and mutation.

The method was developed by John Holland in 1975, although it was popularized later by one of his students, David Goldberg. The work of De Jong in 1975 showed the usefulness of the GA for function optimization and made the first concerted effort to find optimized parameters of the Genetic Algorithm.

In a Genetic Algorithm, successive **populations** of individuals are created. An **individual** is also called a **chromosome** in the GA nomenclature, and is formed by a set of variables (binary variables or real variables) which are called **genes**.

Basically, there are two most important Genetic Algorithms. The difference between them is the way that the individuals (also called chromosomes) of the population are encoded [3] as it is explained in the following figure:

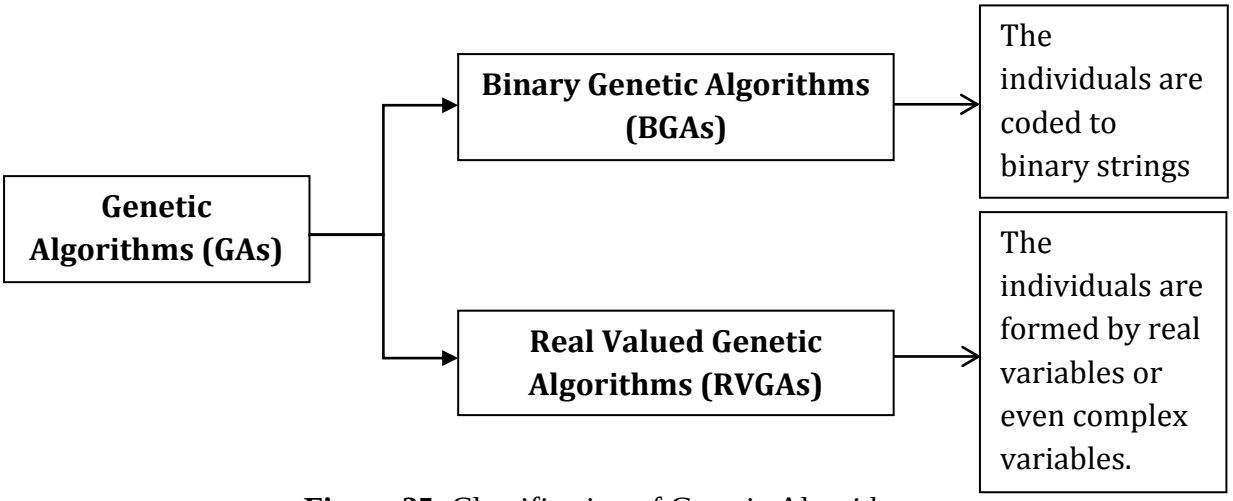

Figure 25: Classification of Genetic Algorithms.

BGAs represent the variables (genes) of each individual as binary values, and work with those binary strings to minimize the cost function. In contrast, RVGAs work directly over the continuous variables themselves.

Here we show the general flow char of a generic Genetic Algorithm and then, an explanation of the main properties of these algorithms is given.

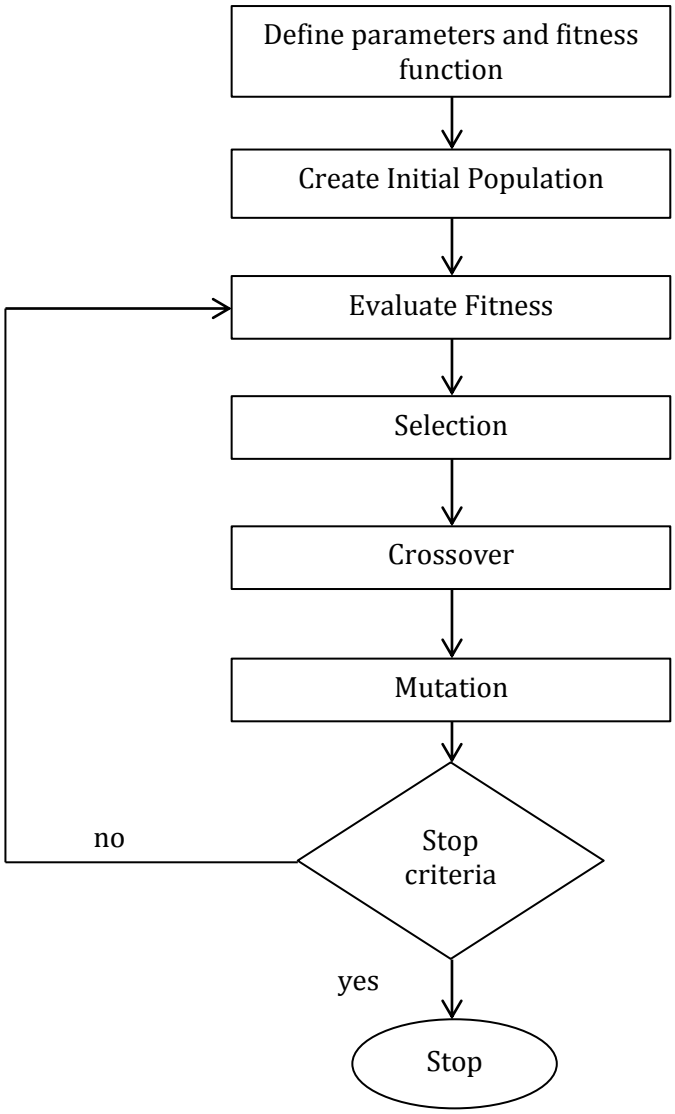

Figure 26: Flow Char of a generic Genetic Algorithm.

4.1.2 Components of a Genetic Algorithm

In this section, the main components and characteristics of the Genetic Algorithm are explained. The most important features to explain from GAs are the selection method, the mating, and the genetic operators, crossover and mutation.

- **Selection**

In each iteration of the algorithm, part of the current population has to be selected to survive and generate new descendants. The portion of the population selected as survivors is relevant in the genetic algorithm performance because it affects the conservation of the genetic information of this population. Normally, the portion of the population selected to survive is that one which best fits the cost function [3]. Therefore, the chromosomes with best cost will be held in the following generation and will reproduce with each other to generate descendants. It is necessary to study which portion of the population is selected to survive and how the number of survivors affects the performance of the algorithm.

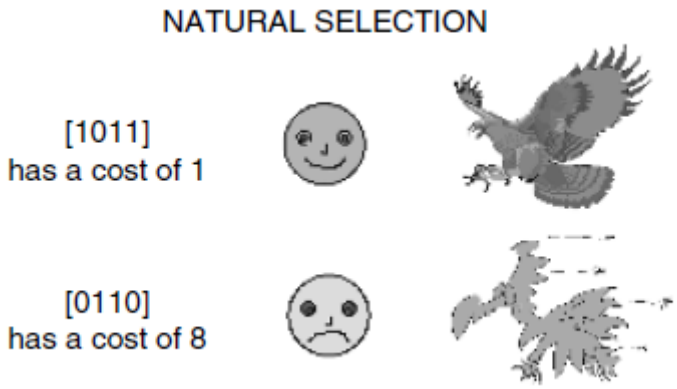

Figure 27: Natural Selection in Genetic Algorithms [Practical Genetic Algorithms, Randy L. Haupt, Sue Ellen Haupt, Figure 2.9]

- **Mating**

The mating is the strategy to select the individuals (chromosomes) to generate descendants. There are several techniques developed for Genetic Algorithms, and the selection of the mating procedure needs to be deeply evaluated, since it has a strong effect in the algorithm performance and convergence. The reader is recommended to go to [3] where a wide description of the different mating strategies is explained.

- **Crossover**

When the survivors are selected and the mating procedure has been done to decide the way the parents are going to mate, crossover is one of the strategies to generate new descendants. Basically, it consists of generating descendants with genetic content of both parents. Part of the genes of one of the parents is going to pass to the offspring, and the rest of the descendant will be filled with the genes of the other parent. To accomplish that, basically one or various crossover points are selected in the parents' chromosomes and the genes between those points are going to be interchanged between the parents to generate the descendant. In Figure 28 and Figure 29, examples of crossover using one single crossover point or two points are represented graphically:

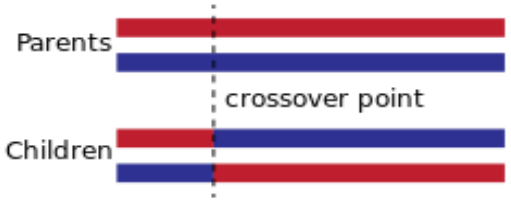

Figure 28: One single crossover point [Wikipedia: Crossover in Genetic Algorithms]

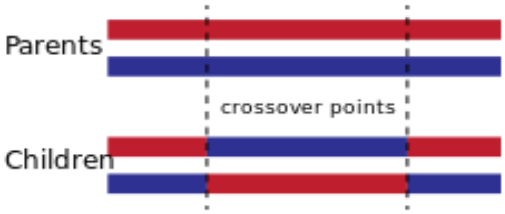

Figure 29: Two crossover points [Wikipedia: Crossover in Genetic Algorithms]

This kind of crossover is widely used in Binary Genetic Algorithms. Nevertheless, whether we have a Real Valued Genetic Algorithm, also called Continuous Genetic Algorithm, by doing the last procedure, crossover is only an interchanging of real numbers among the chromosomes and new genetic information is not added in the following generation. For that reason, other kind of crossover is usually implemented when using the Continuous Genetic Algorithm: Linear Crossover. Linear Crossover lets to produce a new descendant from two selected parents by applying a linear combination of the genes of those parents. Therefore, the offspring contains new genetic information which has been created from the information of the parents. The linear combination of the genes in the progenitors is implemented by using linear equations. The reader is recommended to go to [3] for a better understanding of the concept of linear crossover.

- **Mutation**

The second genetic operator is mutation. If no care is taken, the convergence of the genetic algorithm can be too fast and the algorithm can get stuck in a local minimum, which means that a deceptive solution will be the result [3]. In order to avoid that, it is necessary to increase the genetic diversity of the population so that the algorithm slows down the convergence and an improvement of the performance is achieved. Mutation lets us to modify the genetic information of some chromosomes in the current population so that the diversity is increased; nonetheless, it is not advisable to perform a too high rate of mutation; otherwise the algorithm convergence can slow down and increase dramatically the number of iterations until the optimum value of the cost function is reached or even it can bog down the algorithm.

An example of mutation in the Binary Genetic Algorithm is as follows:

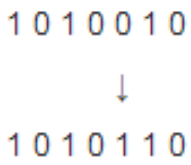

Figure 30: Example of mutation in the Binary Genetic Algorithm

In Figure 31, an example of crossover and mutation operators in Real Valued Genetic Algorithm is shown:

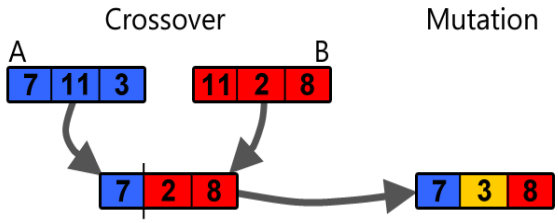

Figure 31: Example of crossover and mutation in the Real Valued Genetic Algorithm

On the other hand there are many other parameters that affect the Genetic Algorithm performance. For instance, the size of the population (number of individuals) the size of each individuals or chromosome, the kind of mating strategy carried out, the number of chromosomes to cross or the number of chromosomes to mutate.

4.2 Application of the Genetic Algorithm to the Phase Retrieval Method

Here, the application of this Genetic Algorithm to the problem with which we are dealing is explained.

As it was pointed out in Chapter 3, the Genetic Algorithm will work directly with the field over the antenna aperture, so that in each iteration of the algorithms which were explained in Chapter 3, the Genetic Algorithm optimize this field in order to find a suitable initial description of the antenna aperture distribution.

In the following table, we establish the association among the concepts that we have studied about Genetic Algorithms and the concepts that we use in the problem of the phase retrieval from the amplitude data.

Genetic Algorithm nomenclature	Phase Retrieval from Amplitude Data
Population	A number (referred to as the population size) of different complex field distributions over the antenna aperture.
Individual or chromosome	Each of the field distributions in each iteration that can be the optimal initial estimation of the field over the AUT.
Genes	The complex points of each possible field distribution over the AUT. One gene has information of amplitude and phase.
Solution: when maximum number of iteration has been made the individual with the lowest cost function.	Solution: when maximum number of iteration has been made the complex field over the aperture with lowest cost function is the initial guess for the Fourier Iterative Algorithm.

Figure 32: Relationship between the Genetic Algorithm concepts and the problem of Phase Retrieval

4.3 Properties of the Genetic Algorithm applied to the problem

Now, the main characteristics of the Genetic Algorithm programmed to find the initial estimation of the field over the antenna aperture are explained.

4.3.1 The initial state

Whether previous information about the complex field over the antenna aperture is known, the initial state of the Genetic Algorithm can be adjusted to speed up the algorithm convergence. Nevertheless, we are not supposed to have any access to previous knowledge of the antenna field distribution, hence the initial guess will be a completely random distribution.

The initial population must be diverse in order to be spread over the entire search domain [20]. This increases the possibility of finding the global minimum of the function. In the following Figure, the different factors that we have to take into account when the initial population is created are indicated:

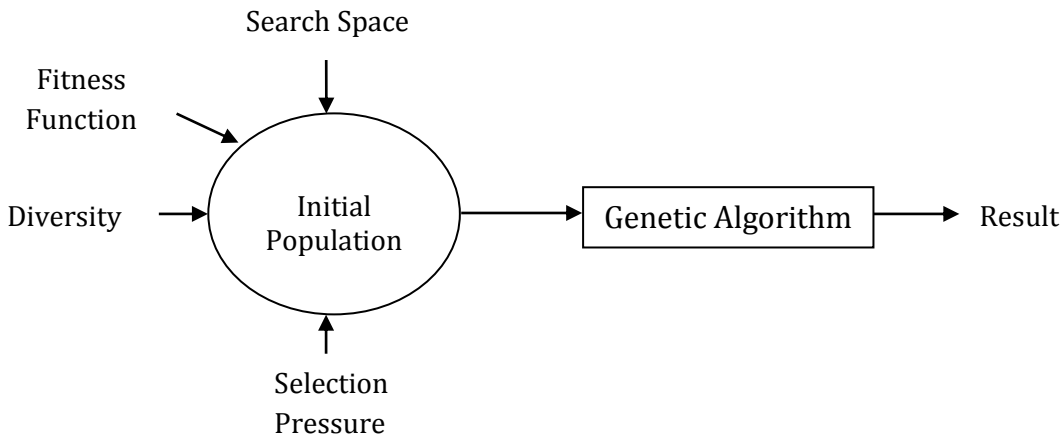

Figure 33: Factors to take into account when programming the initial population in GA

Each individual in the Genetic Algorithm will have a great diversity rate. That means that, for each chromosome, the amplitude values of the genes are going to be different. The procedure to achieve that is given below:

1. We find the boundaries between which the amplitude of each gene can be set.
2. We define intervals between those boundaries, as many intervals as genes are in a chromosome.
3. We define a random value between the previous boundaries for each interval, so that the random value will be located between the numerical limits of each interval.
4. Finally, we assign randomly each amplitude to each gene.

Other thing we have to take into account is how to set the limits of the amplitude values with the information that we have. We only have the amplitude measurements of the field over the two scanning planes. Therefore, it was decided that the highest boundary is going to be the maximum value of the amplitude over the first scanning plane and the lowest value is going to be zero.

Regarding to the phase distribution, since no previous knowledge of the phase is known, each aperture will have a constant phase at the beginning. The phase for each aperture will be a random value between –pi and +pi.

4.3.2 The Selection of survivors

At this point we have to decide how many individuals of the previous generation survive and pass to the next generation to create descendants. It was decided to keep as survivors the 50% best individuals of each generation (the best individuals are those whose cost is lower) and eliminate the rest of individuals. In the following Figure, the procedure of the selection of individuals is graphically represented:

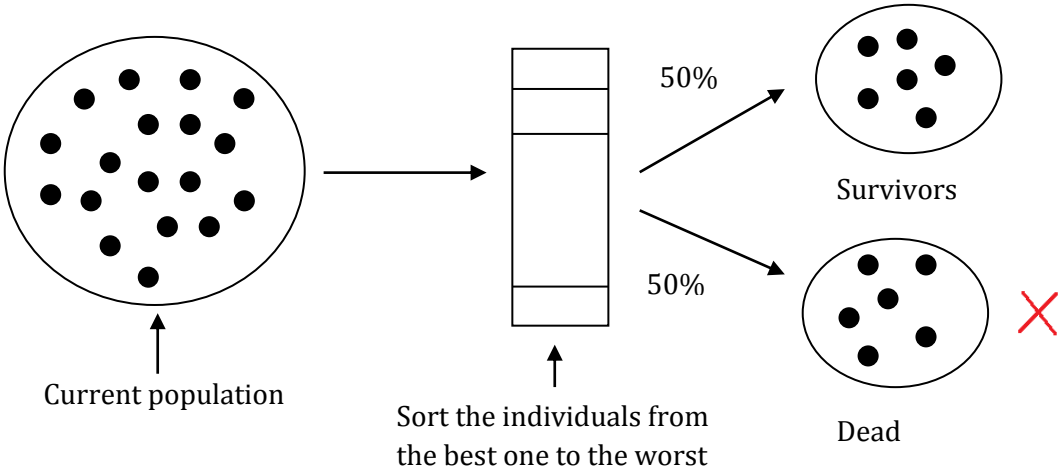

Figure 34: Selection of the 50% best individuals

The portion of population that survives is an important factor we have to decide when programming a Genetic Algorithm. Letting only a few chromosomes survive to the next generation limits the available genes in the descendants. In contrast, if we let too many chromosomes to survive to the next generation we give the bad genetic information more chances to propagate to successive generations and it can slow down the algorithm convergence. For that reason, a selection rate of 50% was chosen. Within this 50% of survivors, 80% generate descendants by applying crossover and 20% by applying mutation.

4.3.3 The pairing strategies

As it was explained in section 4.1, it is also necessary to decide how to pair the individuals that have survived from the selection process to create descendants. In [3], different pairing strategies are explained in detail. For this particular problem, two different strategies have been implemented: population decimation and tournament selection.

- **Population Decimation**

Population Decimation is one of the easiest ways to program the pairing strategy and is widely used. Basically, the parents are selected from the survivors and they are paired randomly, but taking care of not pairing an individual with himself. Whether an individual is paired with himself, we decrease the new genetic information to pass to the next generation. For this reason, we avoid the self-mating.

- **Tournament Selection**

This strategy mimics the mating competition in the nature. Basically, it consists of randomly picking a subset of chromosomes among the survivors of the current population (for example, two or three chromosomes). Those chromosomes are going to compete with each other to become a parent. The chromosome with the best fitness function (lowest cost) becomes a parent. The procedure is repeated in different rounds until the total set of parents is completed. In Figure 35 the way this mating strategy works is schematically represented:

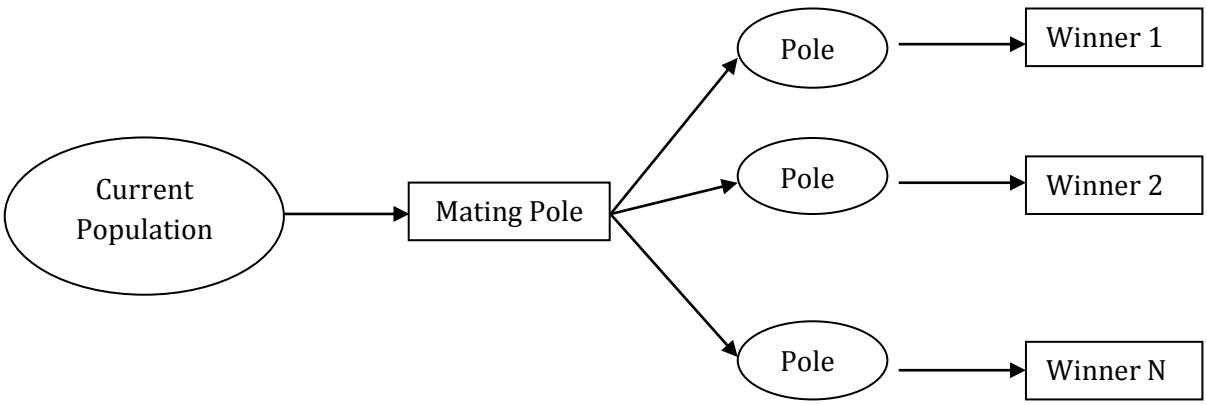

Figure 35: Tournament Selection

4.3.4 Crossover

As it was mentioned above, the 80% of the survivors are going to generate descendants by applying linear crossover. Two descendants are generated from the linear combination of the genes of two parents as follows:

$$parent_1 = [p_{m1} p_{m2} \cdots p_{m\alpha} \cdots p_{mN_{var}}]$$
$$parent_2 = [p_{d1} p_{d2} \cdots p_{d\alpha} \cdots p_{dN_{var}}] \quad (4.1,\ 4.2)$$

$$\downarrow$$

$$p_{new1} = p_{m\alpha} - \beta[p_{m\alpha} - p_{d\alpha}]$$
$$p_{new2} = p_{d\alpha} + \beta[p_{m\alpha} - p_{d\alpha}] \quad (4.3\ .4.4)$$

$$\downarrow$$

$$offspring_1 = [p_{m1} p_{m2} \cdots p_{new1} \cdots p_{dN_{var}}]$$
$$offspring_2 = [p_{d1} p_{d2} \cdots p_{new2} \cdots p_{mN_{var}}] \quad (4.5,\ 4.6)$$

In the previous expressions, the suitable value of β needs to be found. It can be a random value between 0 and 1 or a complex value. An analysis to set the suitable value of this parameter was performed and it is shown in the following chapter, which is dedicated to the simulations and results. On the other hand, it is necessary to set the number of genes that are going to cross in each chromosome. This parameter has been defined by the constant "pc" (the probability of crossover) and it affects to the convergence speed of the algorithm, as it will be shown in the following Chapter.

4.3.5 Mutation

The 20% of the survivors are going to generate descendants by applying the mutation operator. The number of genes that are going to mutate in the selected chromosomes is defined by the constant "pm" (the probability of mutation) and it affects to the convergence as well, as it will be shown in the following chapter.

The implementation of mutation in the Genetic Algorithm is as follows: basically, the genes in the selected parents that are going to be mutated are randomly chosen, and are changed by another random complex values between the suitable limits or bounds so that the chromosome mutated is still inside the search domain. The limits are the same for the initial population, the maximum and the minimum values of the amplitude measurements over the first scanning plane.

4.4 The convergence of the Genetic Algorithm

Before applying the Genetic Algorithm to the problem of the phase retrieval, it is necessary to check whether the algorithm really does what it is supposed to do. We need to guarantee that, of course, the Genetic Algorithm works as a global search procedure and, through some iterations, the algorithm finds the global minimum of a cost function. Once we have checked that our Genetic Algorithm is a well-programmed global optimization method, we can apply it to find the initial guess of the field in the phase retrieval problem.

The cost function selected to check if the algorithm works properly needs to be a "difficult" cost surface, with many local minima, in order to see if the algorithm can get stuck in one of those local minima. The selected function was described in equations (3.1), (3.2) and (3.3), and the cost surface was represented in Figure 14.

Let's see how the Genetic Algorithm makes an initial population of 10 random real variables to converge to the region of the global minimum after a number of iterations. In this simulation, tournament selection has been chosen as the mating strategy, and the probabilities of crossover and mutation (parameters "pc" and "pm") are set to 80% and 10% respectively.

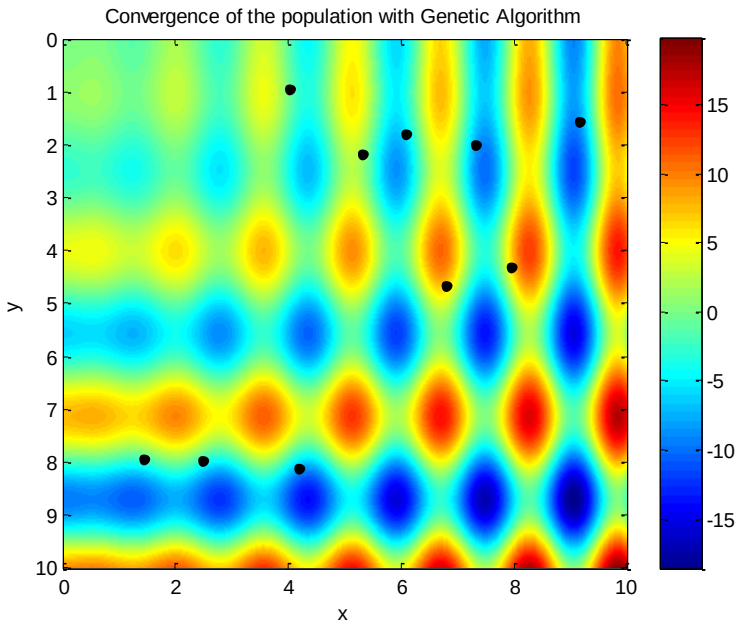

Figure 36: Initial Population of the Genetic Algorithm.

Here we can see what it was pointed out about the initial population. Providing that the initial population is as diverse as possible and it is spread all over the search domain, we improve the performance of the algorithm; otherwise, if the initial population is concentrated in a particular region, it is possible that after applying few times the genetic operators we

reach the stagnation because all the chromosomes reach the same value and the genetic diversity decreases too rapidly without finding the region of the global minimum.

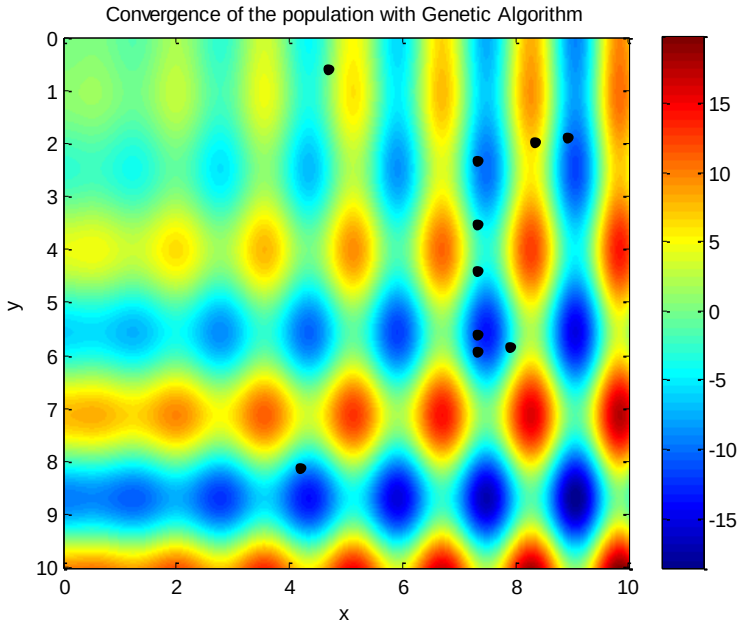

Figure 37: State of the population after 20 iterations

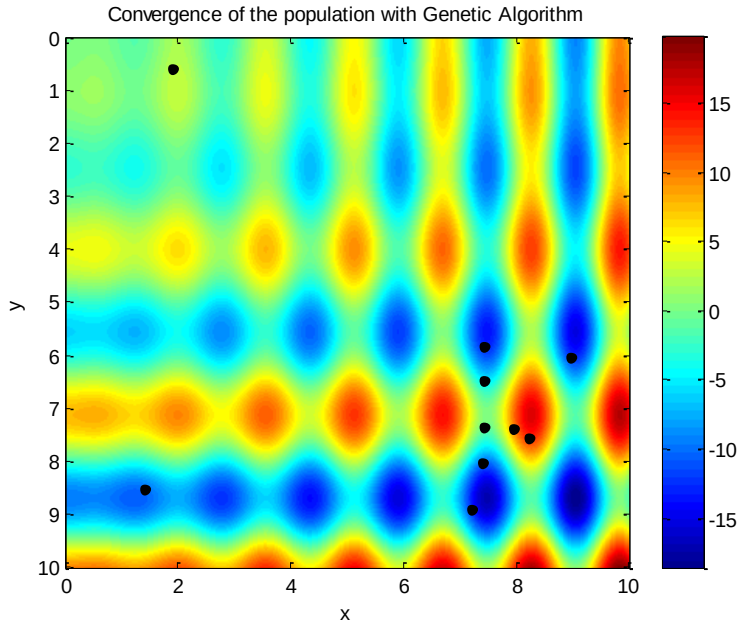

Figure 38: State of the population after 50 iterations.

The genetic operators are applied in each generation over the all population. As we can appreciate, after some iterations the population is converging to the region of the global minimum, looking for the optimal value of the cost function.

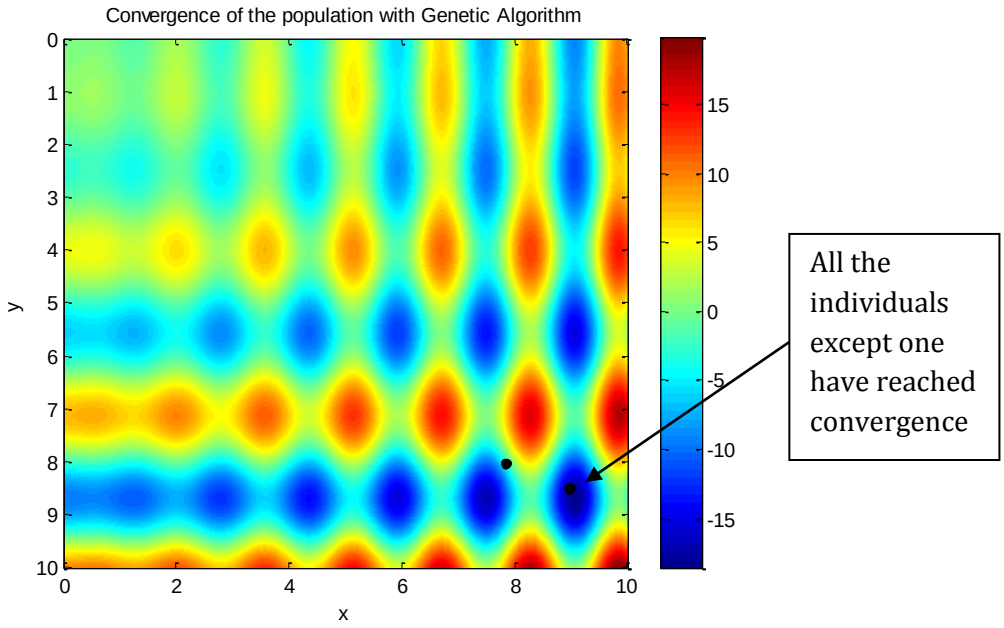

Figure 39: State of the population after 100 iterations.

After 100 iterations, all the individuals except one have reached the state of convergence. The Genetic Algorithm always reaches the global minimum no matters the distribution of the initial population. Therefore, we conclude that the Genetic Algorithm that was programmed works as a global search and, after some iterations, the global minimum of the cost function is found.

5 Simulations and Results

5.1 Simulated data of the analyzed antenna

In this chapter, different simulations have been carried out and the results are shown.

The amplitude data are taken over two planar scanning surfaces located at 3λ and 5λ away from the antenna aperture. As it was pointed out, the architecture used to take the amplitude data is represented in Figure 12(a).

The antenna used during the simulations is a Horn antenna. The dimensions of the Horn antenna aperture are 88 mm for the width and 88 mm for the height respectively. The antenna works at 12 GHz.

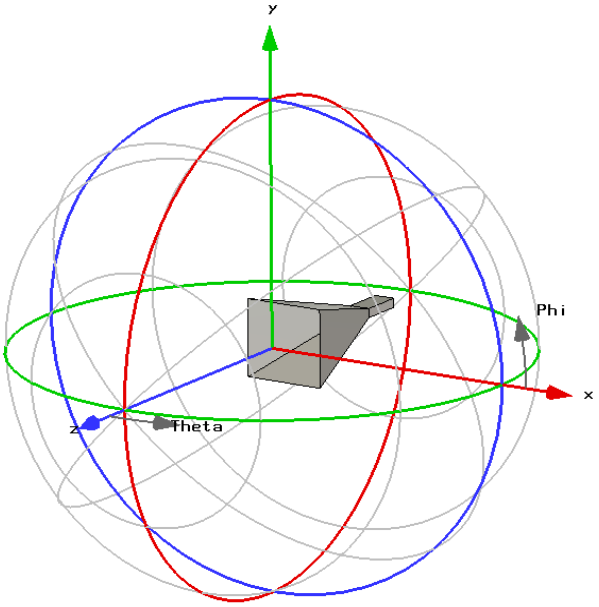

Figure 40: Scheme of the Horn antenna to characterize

The near-field antenna measurement scheme will be described by two scanning planes with the following considerations:

a) The planes are located at 3λ and 5λ respectively. By locating the planes at those positions, we avoid the reactive zone of the antenna and the planes are not far away from the antenna aperture, so that the valid angle is large enough (approximately 60°) .

b) The sample spacing between two sample points is 7.3 mm. Hence, we are satisfying the Nyquist criterion

c) The dimensions of the scanning planes are 38.69 cm for the width and 38.69 for the height respectively.

In the following plots we represent the amplitude measurements of the Horn antenna over the first and the second scanning planes for the X and Y-Component of the field.

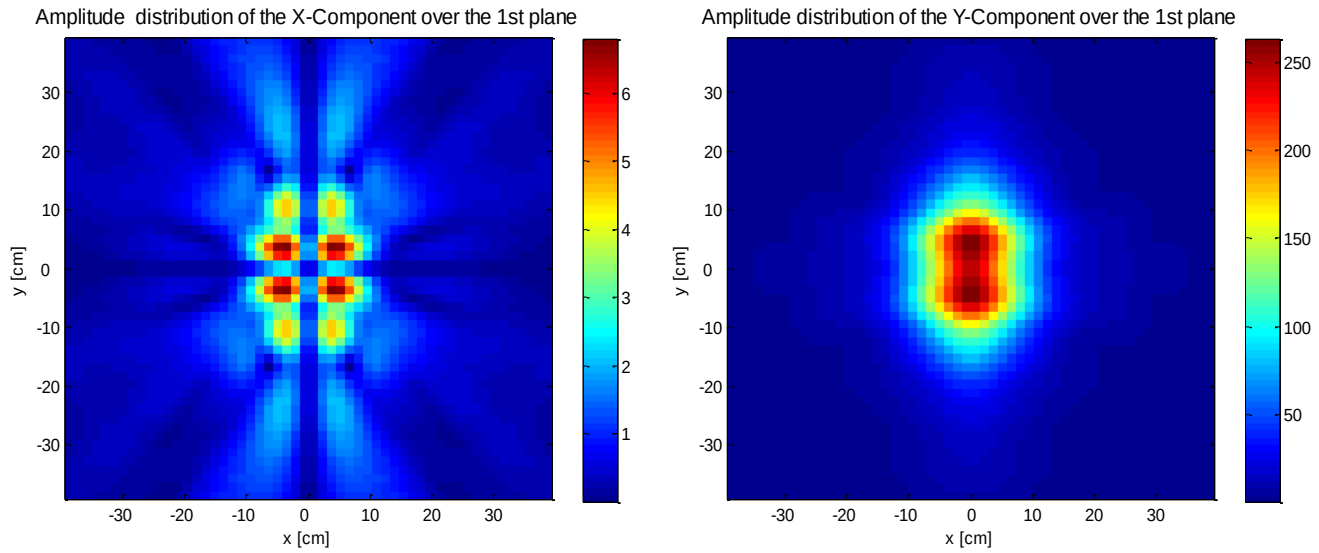

Figure 41: Amplitude distributions over the 1st scanning plane

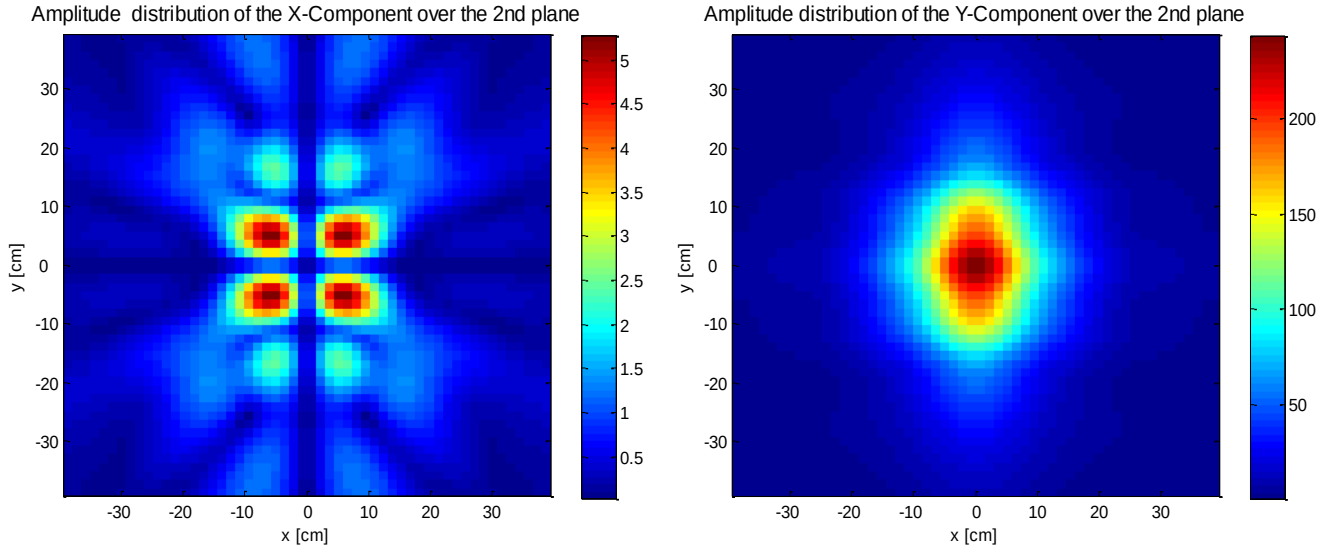

Figure 42: Amplitude distributions over the 2nd scanning plane

And in the following Figures, the far-field radiation pattern of the Horn antenna working at 12 GHz for the main cuts (E-Plane and H-Plane) is also represented.

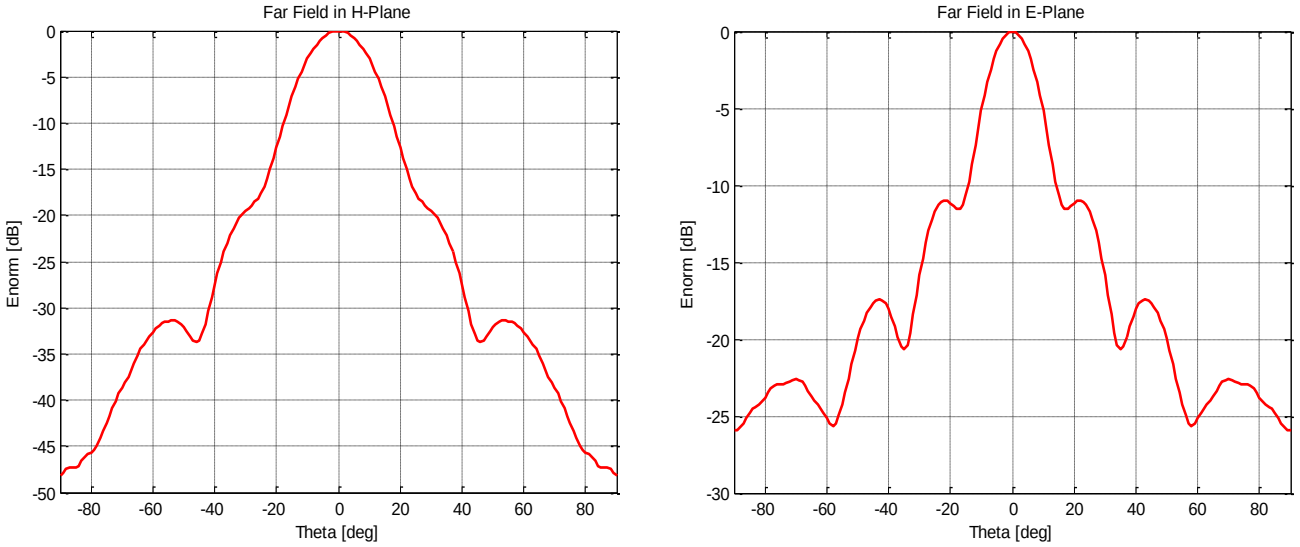

Figure 43: H-Plane and E-Plane of the far-field

5.2 The cost function

Therefore, the reconstruction of the above main planes of the far-field radiation pattern is our goal during the development of this thesis.

During the phase retrieval method, the cost function that has been selected is the following one:

$$F = \sum_{i=1}^{N}\sum_{j=1}^{N}\frac{\left[|E_1(i,j)|^2 - \tilde{M}_1(i,j)^2\right]^2}{\tilde{M}_1(i,j)^2} + \sum_{i=1}^{N}\sum_{j=1}^{N}\frac{\left[|E_2(i,j)|^2 - \tilde{M}_2(i,j)^2\right]^2}{\tilde{M}_2(i,j)^2} \quad (5.1)$$

where E1 and E2 are the calculated amplitudes of the electric field propagated to the first and the second plane respectively, and M1 and M2 are the amplitude measured (obtained from simulations of the Horn antenna in CST) over both scanning planes. This cost function has been widely used in the phase retrieval problem by other authors, [4] and [5]. In this thesis, the cost function has not been studied in terms of stability and other factors. According to the results obtained from other studies [4], [5], this function has good convergence properties, and for a relatively small number of variables, the function converges fast. Whether the number of variables increases, the studies affirms that this cost function presents problems of stagnation. Nonetheless, for this particular small antenna, the number of variables is not too large, and this cost function converges suitably, as we will see in the simulations.

5.3 Results using the first method of the phase retrieval technique.

In this section, the results of the simulation using the first method to reconstruct the phase from the amplitude data taken over two scanning planes are shown. As it was explained in Chapter 3, with this method the initial estimation of the field over the antenna aperture is found by using a Global Optimization procedure based on a Genetic Algorithm. The procedure that we have followed is described in the flow char of Figure 18. The Global Optimization that we use in this section is described in the flow char of Figure 19. Then, once we have the initial estimation of the field over the antenna aperture, we feed the Fourier Iterative Algorithm, and finally, when the phase retrieval procedure is finished, we apply the near-field to far-field transformation in order to achieve the far-field radiation pattern.

5.3.1 General Results of the procedure

The Global Optimization based on the Genetic Algorithm will be the first step. The population of the Genetic Algorithm is set to 30 individuals. The mating strategy selected for the simulations is tournament selection, and the probability of crossover and mutation are set to 0.8 and 0.1 respectively.

In the following figure, Figure 42 we represent how the cost function is minimized by the Global Optimization procedure based on the Genetic Algorithm for a total of 10.000 iterations.

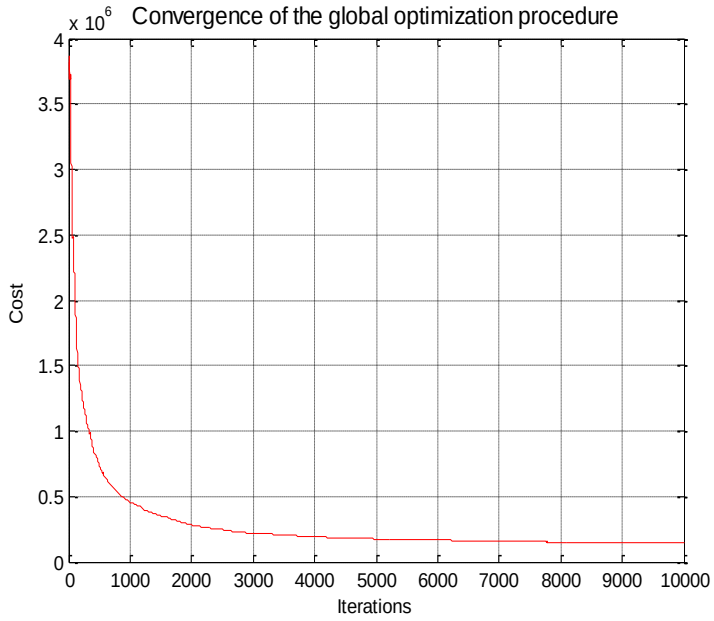

Figure 44: Convergence of Global Optimization for 10.000 iterations.

In Figures 45 and 46, the reconstruction of the amplitude from the initial estimation of the field on the 1st scanning plane is also shown for the x and y-components of the field.

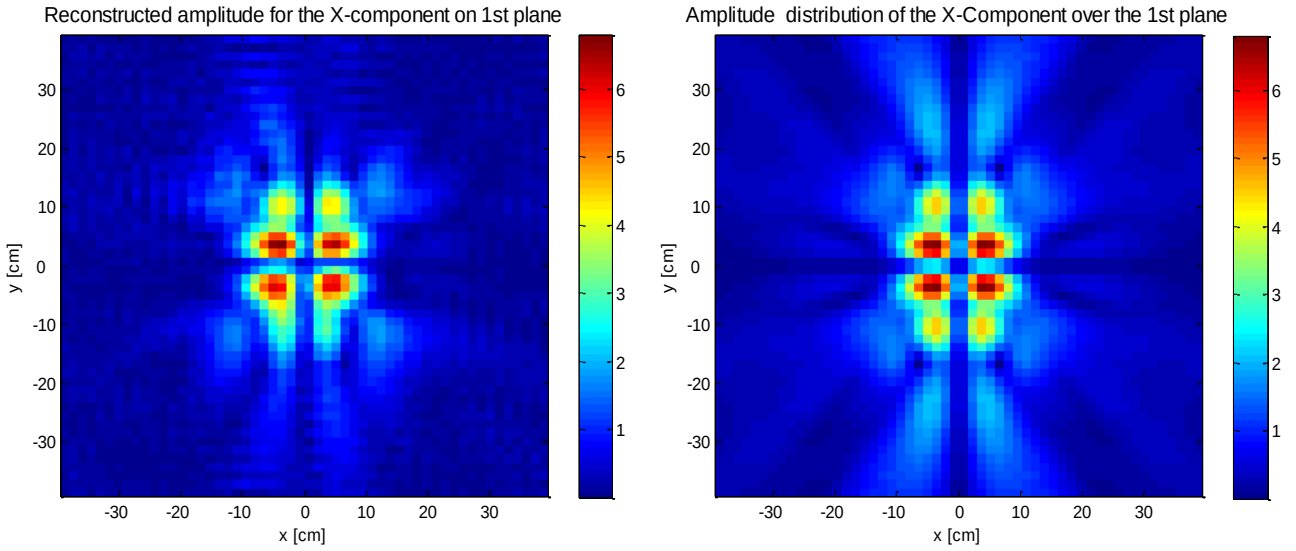

Figure 45: Reconstructed amplitude for the X-Component over the 1st plane

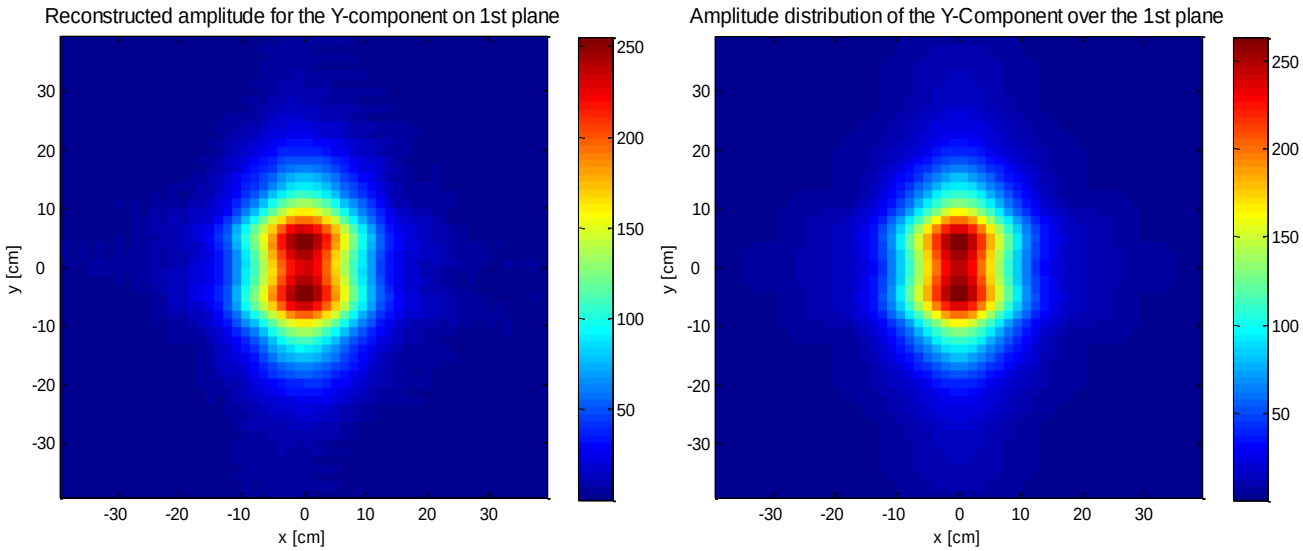

Figure 46: Reconstructed amplitude for the Y-Component over the 1st plane

The reconstructed amplitudes of the previous figures were obtained by propagating the initial estimation of the field over the antenna aperture obtained by applying the Global Optimization to the first scanning plane. As we can see, this initial estimation minimizes the difference between the calculated and the measured amplitudes over the planes and this estimation is now closer to the real field distribution over the antenna aperture.

In Figure 47 and Figure 48 we can see how the reconstruction of the phase distribution over the first scanning plane is. The real phase distribution of the Horn over the plane was obtained by simulations in CST. As it was done for the amplitude, the initial estimation was propagated to the first scanning plane and the phase was obtained. In the following figures, the phase for the x and the y-component of the field over this first plane is shown:

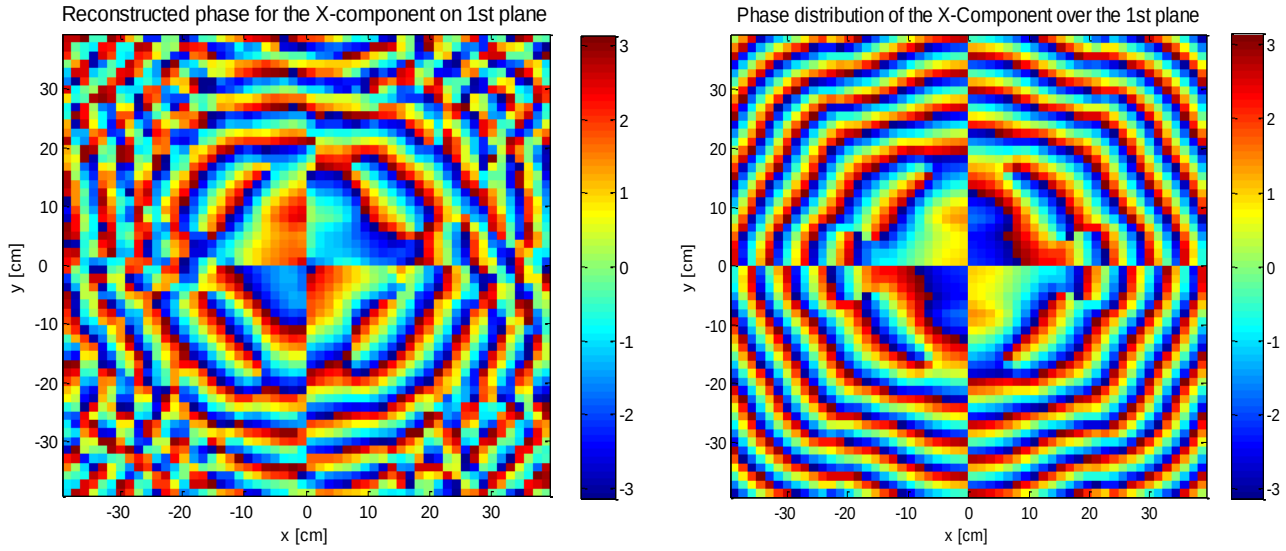

Figure 47: Initial estimation of the phase over the 1st plane for the X-Component

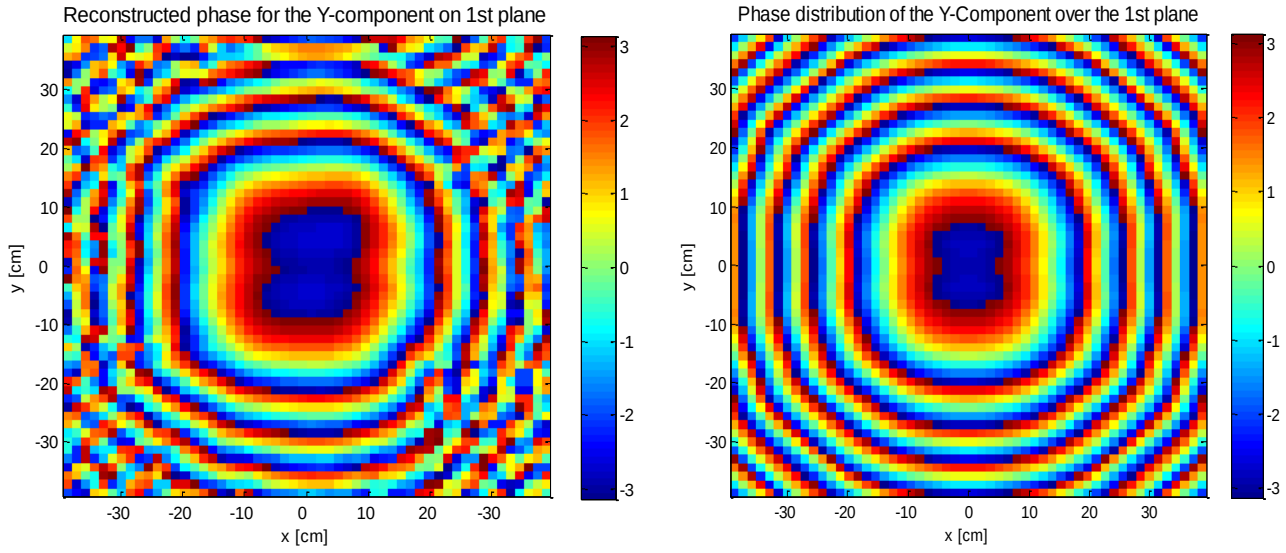

Figure 48: Initial estimation of the phase over the 1st plane for the Y-Component

After getting this initial estimation of the field, the Fourier Iterative Algorithm is applied. Basically, the Fourier Iterative Algorithm refines the initial estimation of the phase through a number of iterations. Fourier Iterative Algorithm also minimizes the same defined cost function, as we can appreciate in the following figure:

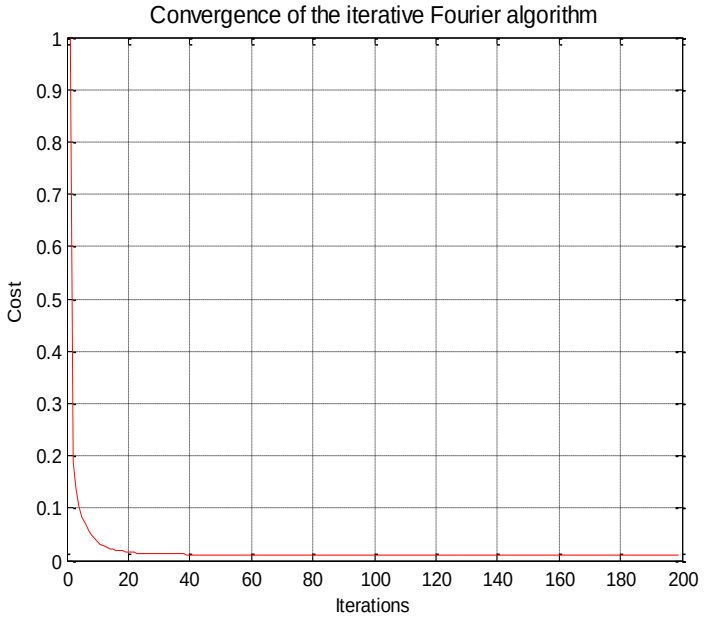

Figure 49: Convergence of the Fourier Iterative Algorithm

When the Fourier Iterative Algorithm finishes, we have a complete characterization of the near-field distribution, with distributions of amplitude and phase. Now, the plane wave spectrum (PWS) over one of the scanning planes can be computed. The first scanning plane was chosen to compute the plane wave spectrum because is closer to the antenna aperture; hence, the valid-angle in the far-field pattern is bigger. When the PWS is obtained, the near-field to far-field transformation is developed as it was explained in the flow char of Figure 8.

In Figure 50 and Figure 51 we can see how the final reconstruction of the far-field radiation pattern is over the two main plains, the H-Plane and the E-Plane. Only the region of the valid-angle (which is described in equation 2.6) is shown. Outside this region, the truncation effect due to the finite dimensions of the plane produces mismatches in the reconstructed far-field radiation pattern, so that this region is not interesting for us.

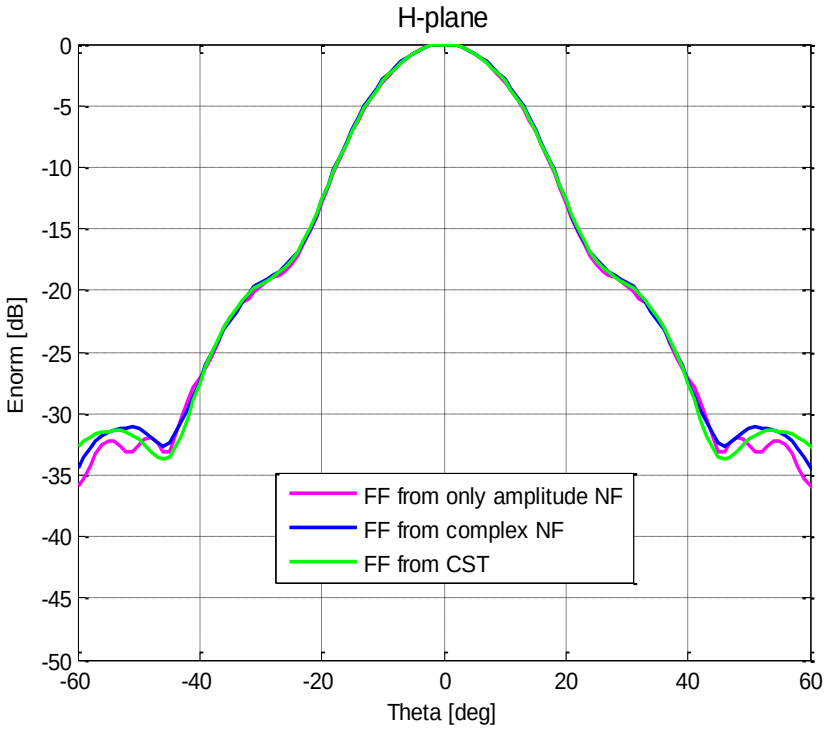

Figure 50: Reconstruction of the H-Plane

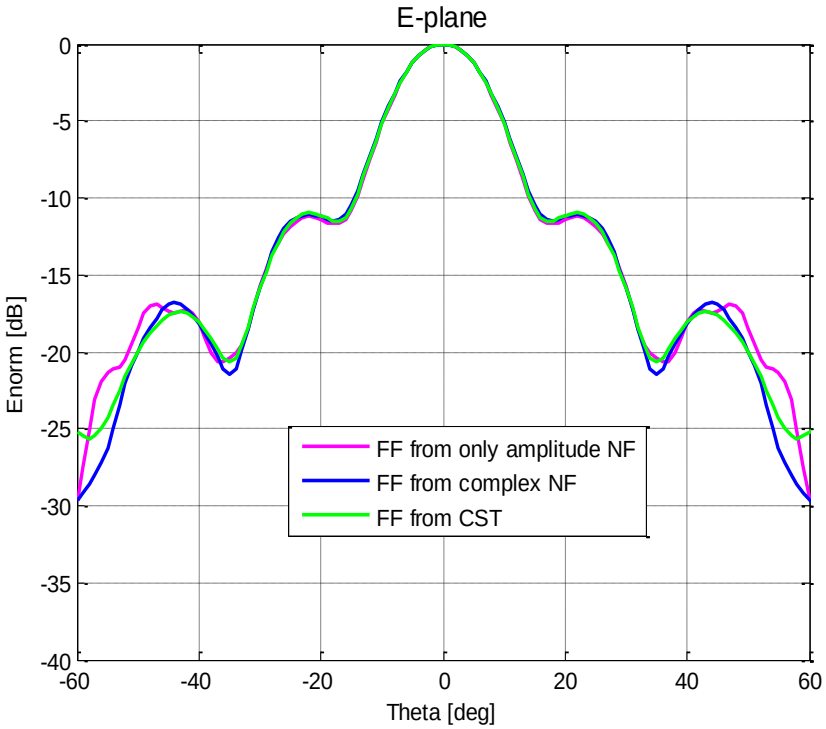

Figure 51: Reconstruction of the E-Plane

In the previous plots, the green function is the far-field obtained from simulations in CST. Therefore, this is our reference. The blue function is the reconstruction of the far-field radiation pattern from complex near –field measurements.

Regarding to the pink curve, it is the reconstruction of the far-field radiation pattern from only amplitude data. Therefore, the pink graph is the result of applying the phase retrieval method from the amplitude data over the scanning planes and the transformation. Only the region of the valid angle is shown.

As can be seen, we obtain a good accuracy in the reconstruction of the far-field. That means that the recovery of the phase from amplitude data was suitable. The criterion that we are going to use to evaluate the performance of the method hereinafter is the difference between the far-field from the CST simulations and the far-field by using our algorithms in both planes. Especially we are going to be focused on the error in the main lobe and in the side lobes, since this is the most important part of the radiation pattern, where the important information of the radiating properties of the antenna is described. In Figure 52, the error is shown for the same planes (H-Plane and E-Plane) of the far-field radiation pattern:

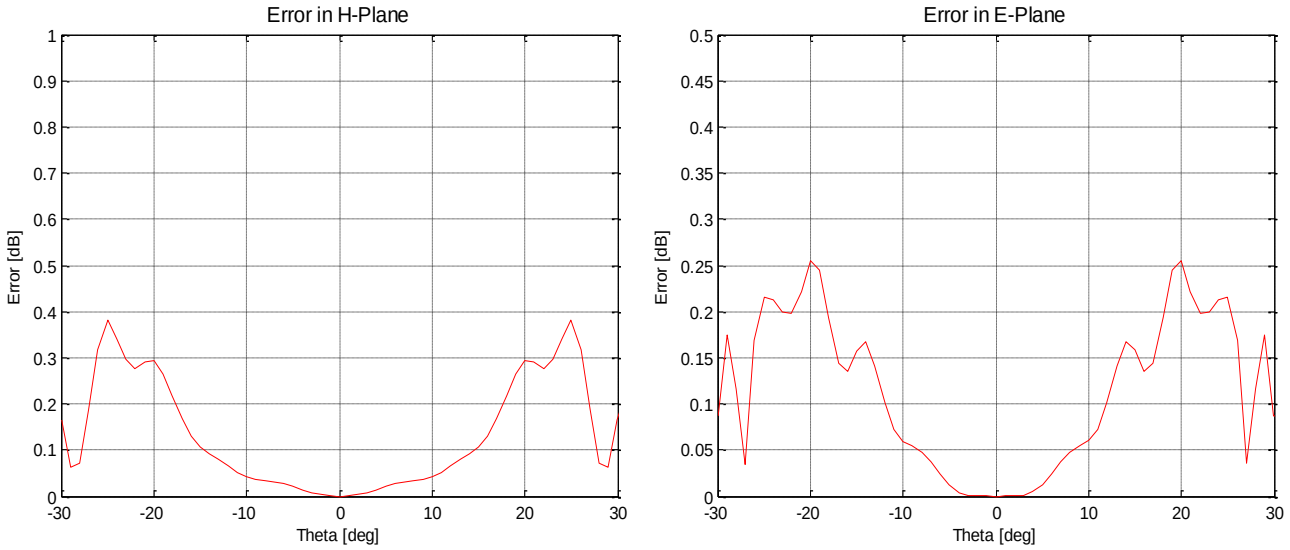

Figure 52: Error in main planes, H-Plane and E-Plane

5.3.2 The comparison with using only FIA

For this particular antenna, it has been found that the Fourier Iterative Algorithm works really well when the suitable number of iterations has been reached. With the iterative technique we obtain a symmetric error in the far-field reconstruction providing that the suitable number of iterations has been reached.

. In Figure 53, the error using the Fourier Iterative Algorithm exclusively and the error using the Global Optimization previously to find an initial estimation of the field over the antenna aperture is compared:

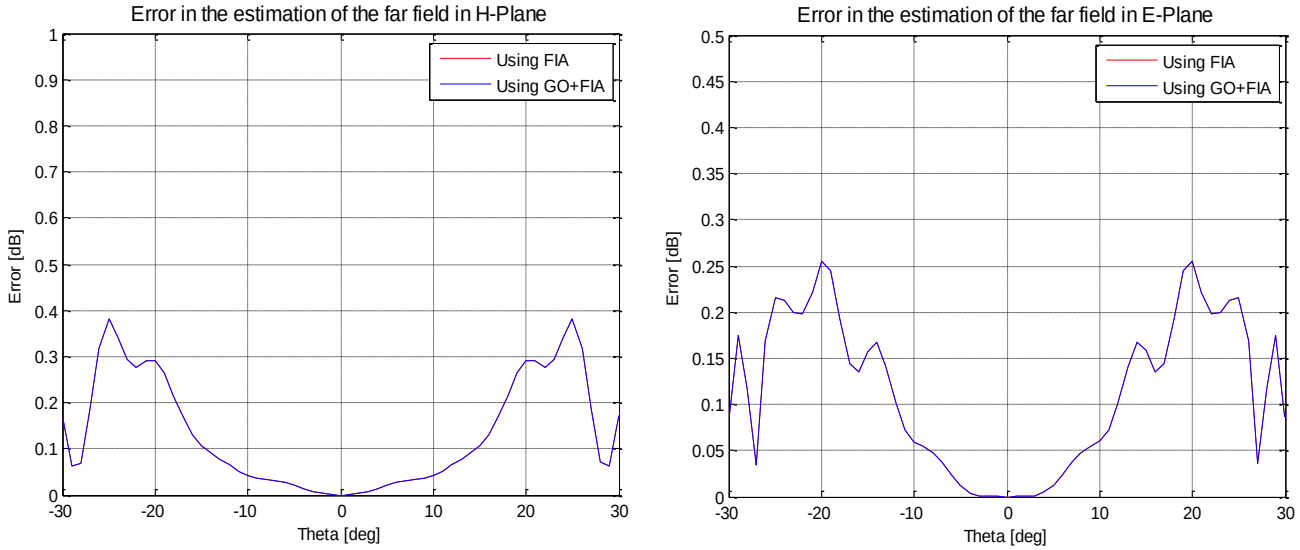

Figure 53: Comparison between using only FIA or FIA+GO when increasing the number of iterations of FIA.

As we can see, there are no differences between using the Global Optimization or not. For this particular antenna, the Fourier Iterative Algorithm works really well for any particularly complex initial guess of the field when the suitable number of iterations has been made. With a number of 500 iterations, is enough for the Fourier Iterative Algorithm to reconstruct with an acceptable level of accuracy the far-field radiation pattern.

Therefore, it seems to be that, for this particular antenna, whose radiation pattern is not complicated, the iterative technique works properly and the global optimization in order to find an initial guess of the field is not needed.

5.3.3 The asymmetry in the reconstructed far-field radiation pattern

During the simulations it was noticed that, unless a sufficiently high number of iterations of the Fourier Iterative Algorithm is made, in the reconstructed far-field radiation pattern we can see a small effect of asymmetry. If we let the algorithm to converge, the effect of this asymmetry practically can be ignored.

In Figure 54 we can see this effect:

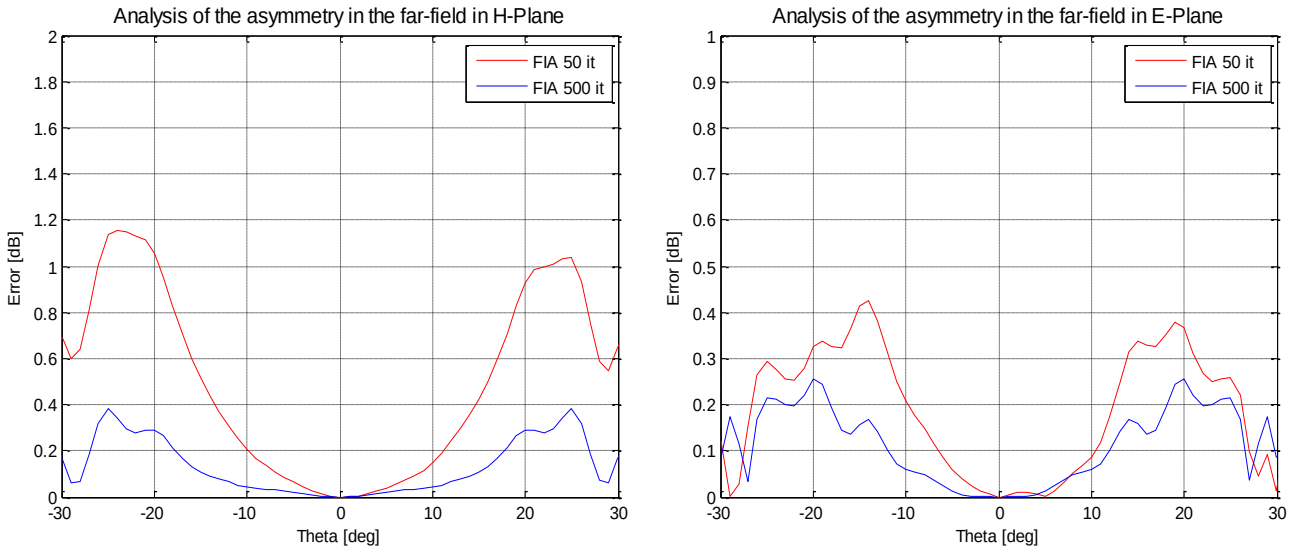

Figure 54: The asymmetry of the reconstructed far-field radiation pattern.

The asymmetry effect always appears when the number of iterations of the Fourier Iterative Algorithm is not high enough. For more than 100 iterations, this asymmetry effect disappears For a lower number of iterations, even when the Global Optimization is used, the asymmetry effect is presented and, as we will see a bit later it produced problems to understand some simulations.

5.3.4 The Selection of the Genetic Parameters

Basically in this section the selection of the Genetic Operators is going to be explained. When the Genetic Algorithm is programmed, parameters such as the population size, the pairing strategy, or the importance of crossover and mutation have to be considered. In our case, we studied the influence of those parameters by evaluating to two criteria: the convergence speed of the Global Optimization, and the influence on the accuracy of the far-field. For all of the simulations, the optimizations were repeated 30 times and the average results are presented in this document.

- **The influence on the convergence of the Global Optimization**

The Population Size

Different population sizes were studied and the following results were obtained:

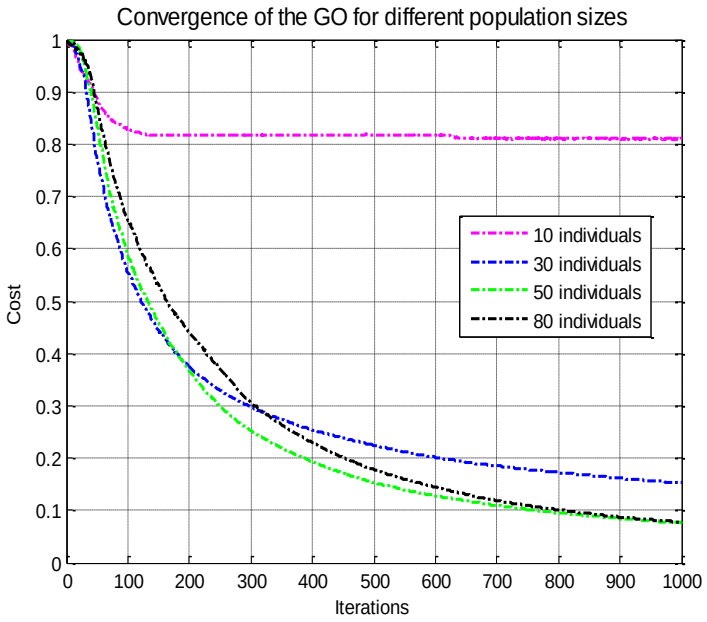

Figure 55: Convergence speed of the Global Optimization for different population sizes.

As we can see, for small populations such as 10 individuals the algorithm stagnates too fast, and the initial guess of the field over the antenna aperture is not going to be a suitable initial guess. For small populations, the genetic operators (crossover and mutation) have more influence on the diversity and the state where the diversity decreases to zero is reached too soon. When that state is reached, there are not differences between the individuals of the populations, and it produces the stagnation of the algorithm.

The Genetic Algorithm work better for larger populations, for example 50 or 80 individuals. When the population grows the algorithm slow down, of course, since the genetic operators and transformations have to be applied over more individuals. For that reason, the rest of simulations where developed with a standard population of 50 individuals.

The Mating Strategy

Two mating strategies were programmed: population decimation and tournament selection, and the influence on the convergence speeds of both of them were studied:

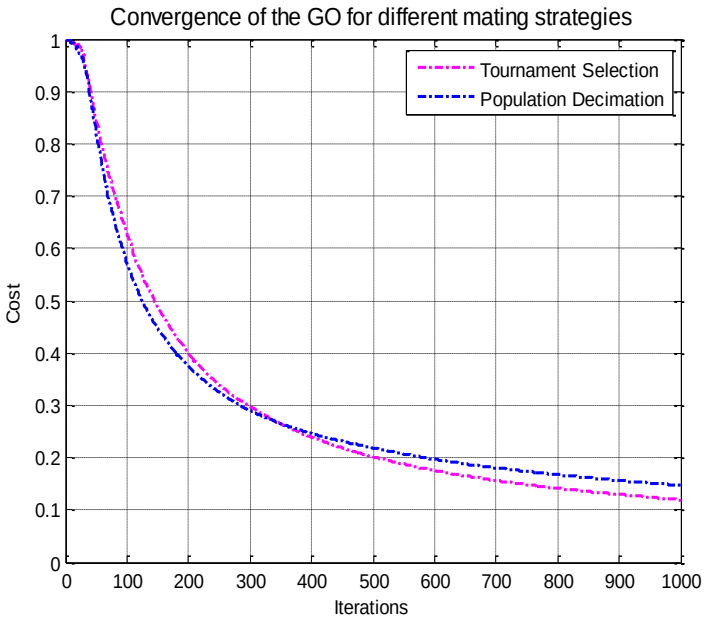

Figure 56: Convergence speed of Global Optimization for different mating strategies.

With tournament selection, the best pairs of chromosomes in each iteration are formed, while in population decimation the survivors are paired randomly. Tournament Selection preserves better the good genetic information and we obtain a lower cost.

The Crossover Rate

As it was pointed out in Chapter 4, the crossover rate is the portion of genes of the selected chromosome that are going to be crossed using equations (4.1)-(4.6). This portion is referred to as "pc".

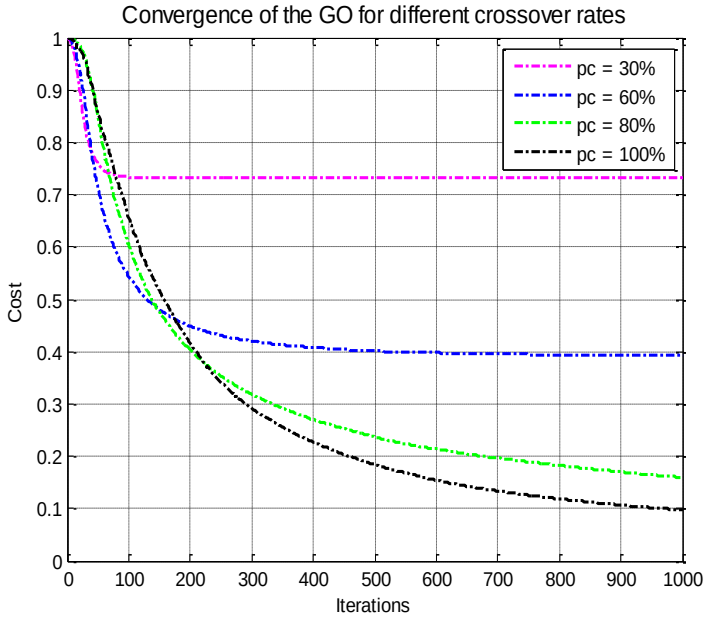

Figure 57: Convergence of Global Optimization for different crossover rates.

Crossover is the most important genetic operator and the responsible for changing the genetic information when a new generation is going to be created. If the crossover rate is too low, the algorithm can slow down, or even bog down since the change is too slow, as we can appreciate for a crossover rate of 30%. High crossover rates have been used for all of the simulations, such as 80% or 100%, since the algorithm present a better performance.

Crossover is implemented by using the linear equations (4.3) and (4.4). It was seen that the definition of the parameter β is quite important and affects significantly to the convergence of GO. This parameter is always a random value between [0,1], so that we guarantee that the new chromosome is between the defined boundaries for the individuals. An study about the influence of this parameter was developed, by fixing the value to 0.5, or using a random real value between [0,1] for each chromosome or using a random complex value.

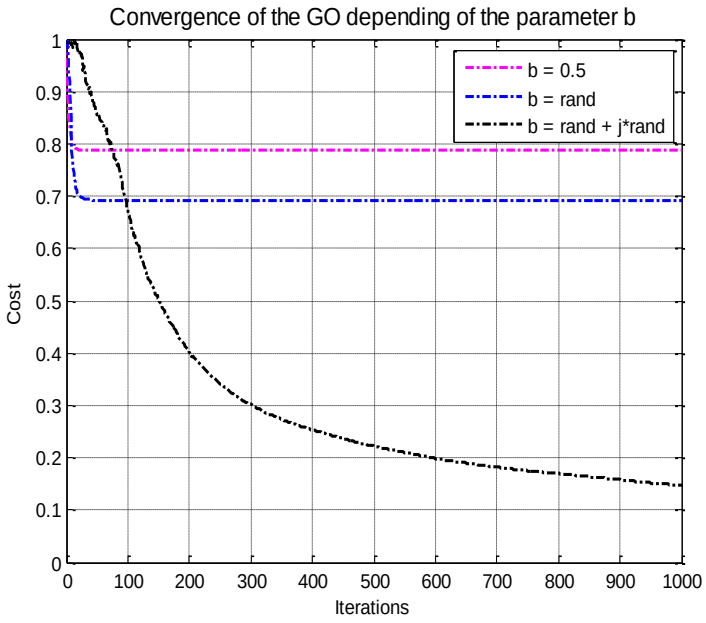

Figure 58: Convergence of Global Optimization for different β-parameters

At the beginning, the real values for β were used. As we can see, the algorithm stagnates too fast if real values of β are used. Nonetheless, when a complex random value is used, the performance of the algorithm improves. The complex value adds diversity to the population; since the genes of the chromosomes are actually complex values, if β is a real parameter crossover simply implements recombination of genes, and it causes the too fast convergence. Consequently, all the simulations were performed by using a random complex value of β for each chromosome that is going to be affected by crossover.

The Mutation Rate

When a new population is going to be created, the 20% of survivors are going to generate descendants by mutations. The number of genes that are going to be mutated in those individuals respect the entire chromosome is referred to as "pm", and also affects the convergence speed of the Global Optimization.

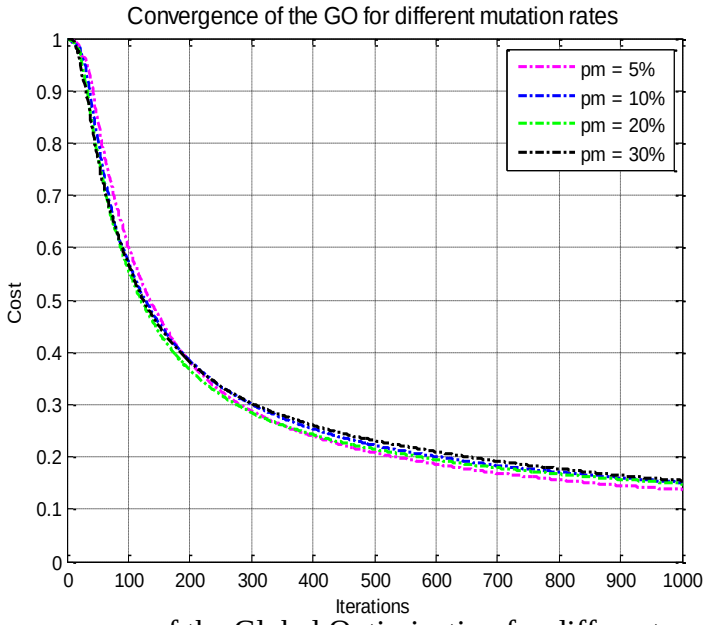

Figure 59: Convergence of the Global Optimization for different mutations rates.

Mutation adds new abrupt genetic information in each generation so that the algorithm tries to avoid the local minima. Usually, low rates of mutation are used (for example, 5%); otherwise, the mutation can slow down the convergence.

- **The influence on the accuracy of the radiation pattern**

It was explained in section 5.3.3 that, if we stop the Fourier Iterative Algorithm before the convergence of the algorithm, we can see when we reconstruct the far-field radiation pattern a small effect of asymmetry on the error. However, by increasing the number of iterations of the iterative technique the effect of the asymmetry disappears.

Owning to this asymmetry, the analysis of the influence of the genetic operators on the far-field radiation pattern is clouded. On the other hand, by increasing the iterations of the iterative technique, this asymmetry effect becomes practically zero. When a sufficient number of iterations is reached, there is not differences between using the Global Optimization or not as it was explained before. The Global Optimization does not enhance the accuracy of the

reconstructed far-field radiation pattern and the Fourier technique always converges with the same accuracy, independently of the initial condition. Therefore, in this case, the effects of the variation of the genetic operators are not appreciable in the accuracy of the reconstructed far-field radiation pattern.

In Figures 60 and 61 some simulations were shown in order to see these effects:

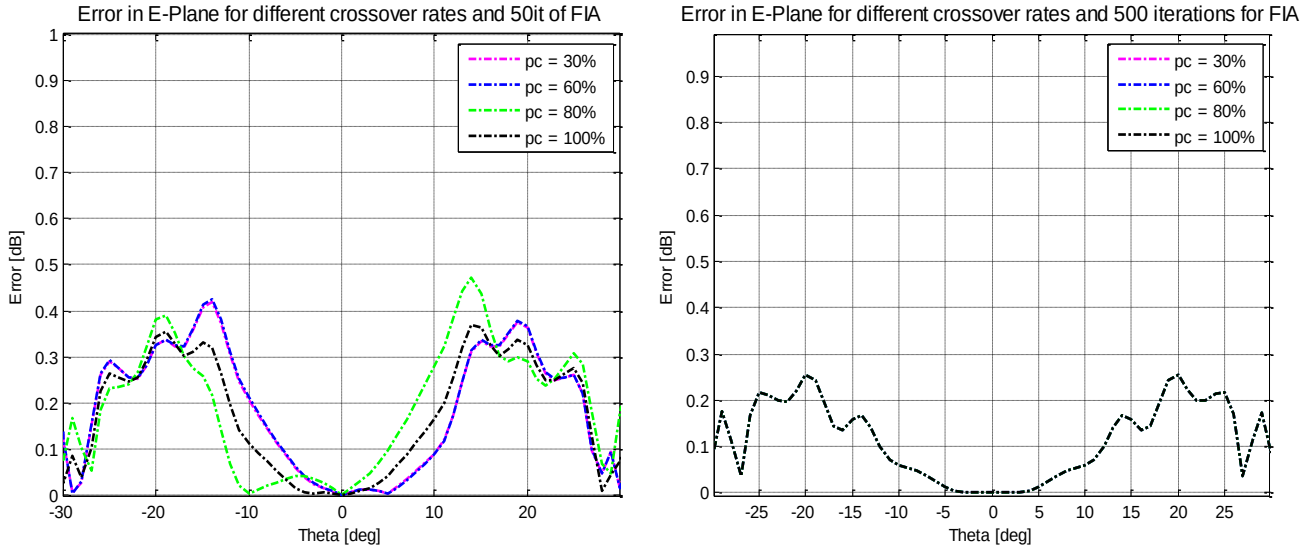

Figure 60: Error in E-Plane for different crossover rates. Left: FIA has 50 iterations. Right: FIA has 500 iterations.

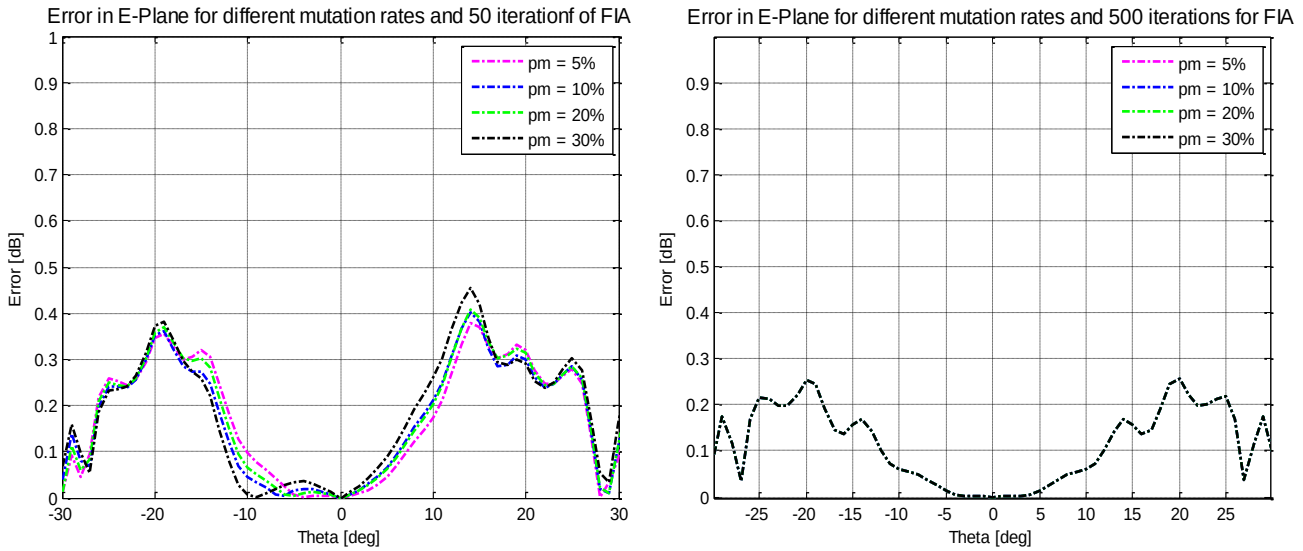

Figure 61: Error in E-Plane for different mutation rates. Left: FIA has 50 iterations. Right: FIA has 500 iterations.

5.4 Results using the second method of the phase retrieval technique

In this section, the reconstruction of the phase from the amplitude data taken over two different scanning planes has been developed by using the second method of the phase retrieval technique. In this method, as it was explained in Chapter 3, the global optimization based on Genetic Algorithm and the Fourier Iterative Algorithm are implemented in the same algorithm (see flow char of Figure 21). In each iteration, the Genetic Algorithm sets an estimation of the field over the antenna aperture. Then, this estimation is propagated to the scanning planes and FIA is applied, minimizing the similar cost function defined on first plane. The field is propagated back to the antenna aperture, where the Genetic Algorithm will work again to establish a new estimation of the field.

5.4.1 Comparison with the first method of phase retrieval

This algorithm has demonstrated to have better properties of convergence than the previous method. Of course, by using the information given by FIA in each iteration over the estimation of the field over the antenna aperture, the algorithm speeds up. In Figure 62 the difference in the convergence speed between the first method and this one is shown:

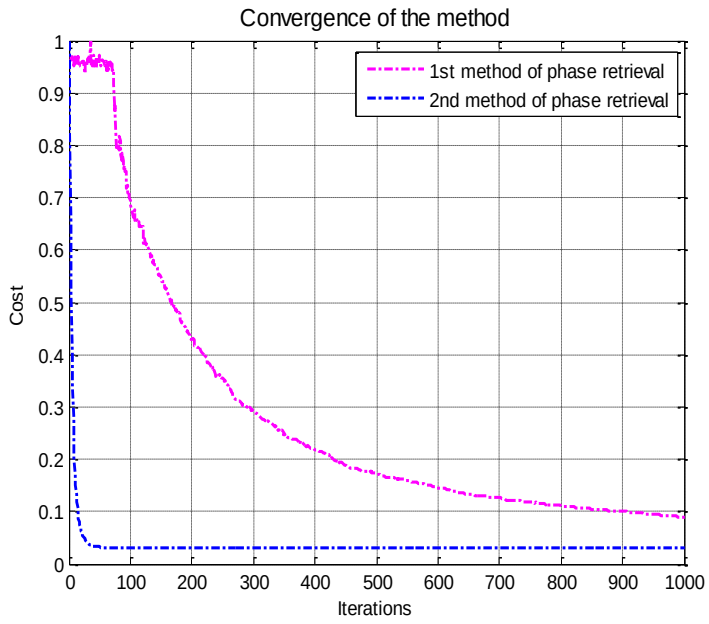

Figure 62: Comparison of the convergence between the first method of phase retrieval and the second method.

Apart of this, the accuracy of the reconstructed radiation pattern is also enhanced by using this second version, as we can appreciate in the following figures:

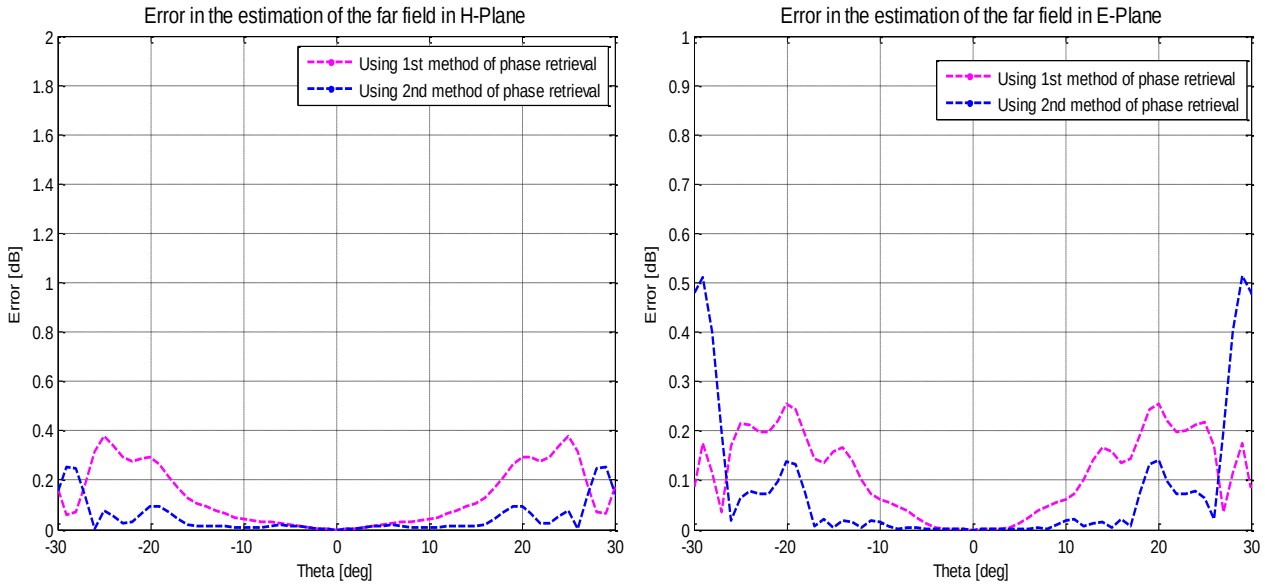

Figure 63: Comparison of the accuracy in the far-field with the first method of phase retrieval and the second method.

With this method, the cost function is evaluated on the first scanning plane. When the algorithm stagnates or we decide to stop the algorithm, we can check how the reconstruction of the field over the first scanning plane is, for example. As we can see in the following figures, Figure 64 and Figure 65, the reconstruction of the amplitude over the first scanning plane in this case is closer to the amplitude distribution that was obtained from the simulations in CST.

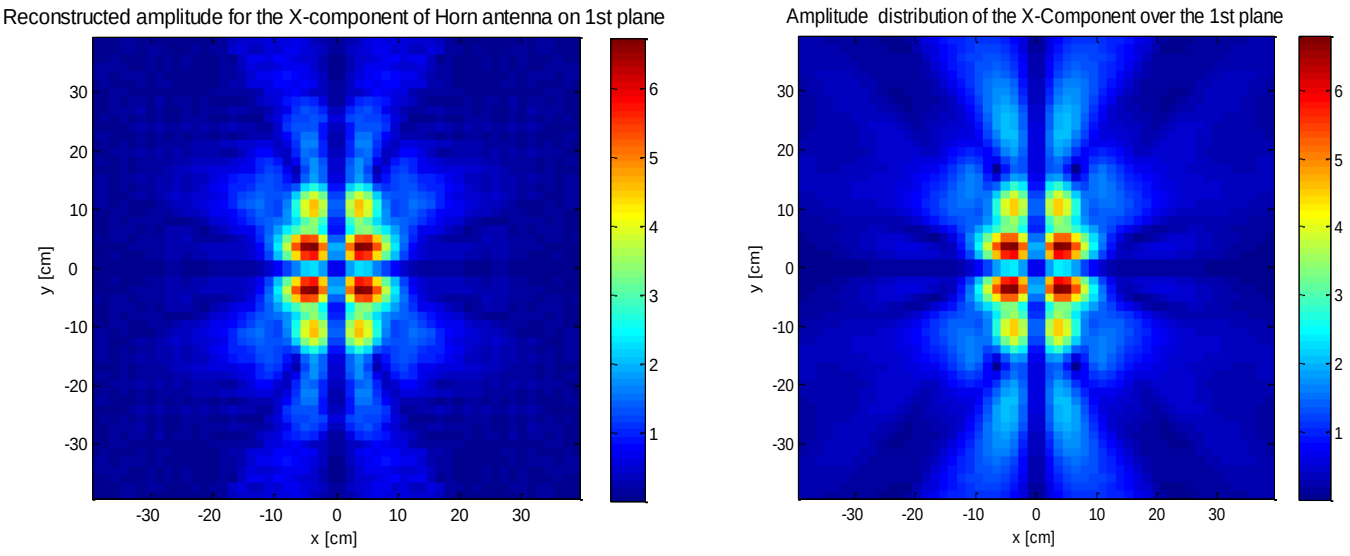

Figure 64: Reconstruction of the amplitude of the X-component over the 1st plane

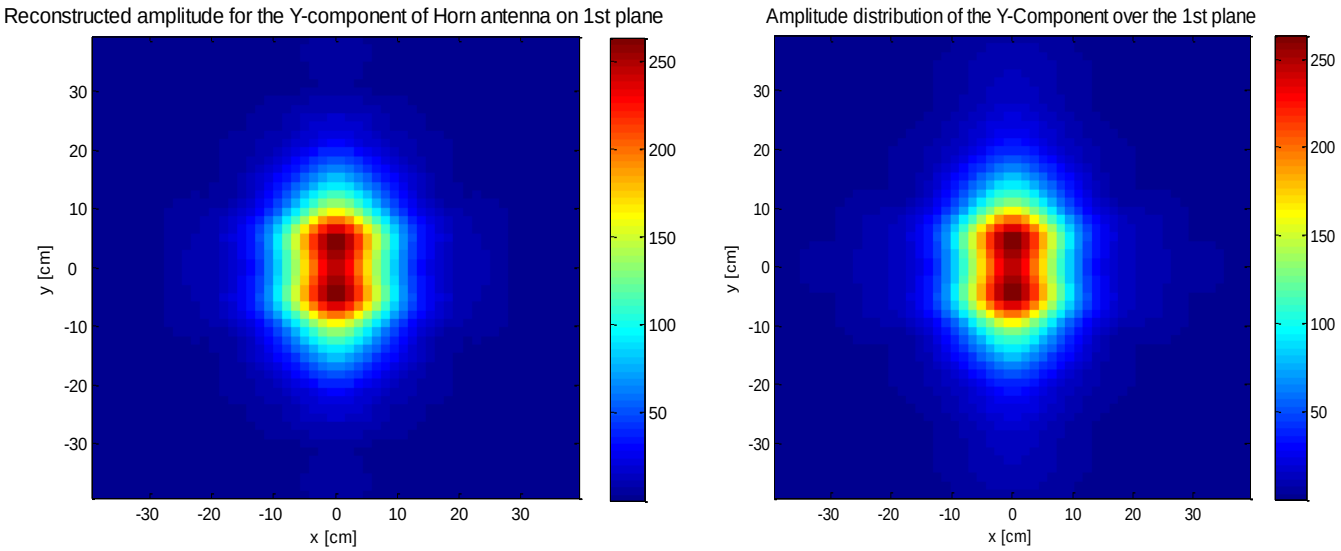

Figure 65: Reconstruction of the amplitude of the Y-component over the 1st plane

Once we have the complex field characterized over the first plane, when the algorithm finishes, it is not necessary to apply again the Fourier Iterative Algorithm, so at the end this method is quite faster than using the Global Optimization and the Fourier Iterative Algorithm separately. Over this reconstructed field over the first plane, the near-field to far-field transformation is applied and the far-field radiation pattern is obtained.

5.3.1 The comparison with using only FIA

As we did with the first method of the phase retrieval, we are going to compare here the accuracy of the reconstructed far-field radiation pattern when this second method is used.

In Figure 66, the valid-angle of the reconstructed far-field radiation pattern is shown by using the second method of the phase retrieval and using exclusively the Fourier Iterative Algorithm. As we can see in this Figure, outside the region of the main lobe and the secondary lobes of the radiation pattern, the second phase retrieval method we are analyzing presents a bigger error than using exclusively the Fourier Iterative Algorithm, although the difference is really small. The biggest difference in this region is about 0.3 dB. As it was pointed out previously, the most important information of the radiation pattern is located in the region of the main and the side lobes, which is between -30 and 30 degrees. For this region, the second phase retrieval method presents better accuracy. In Figure 67, this region is shown in more detail.

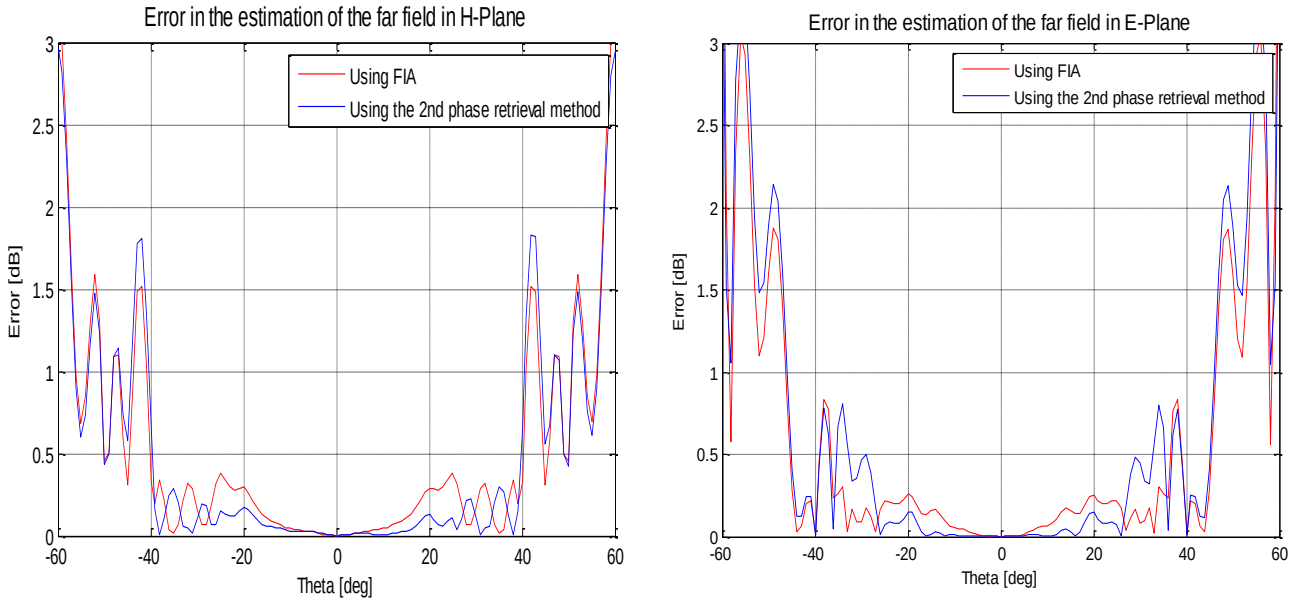

Figure 66: Comparison of the error in the valid region between using FIA and the second phase retrieval method

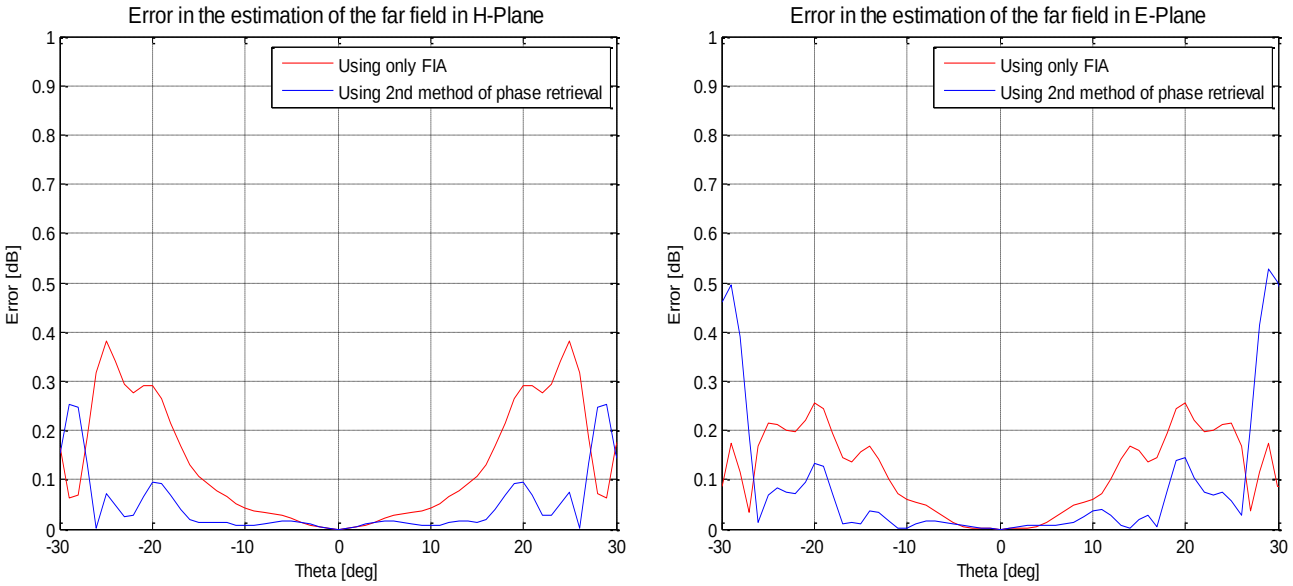

Figure 67: Comparison of the accuracy of the far-field between hybrid method and using only FIA.

Therefore, according to the results, this second method results more interesting for us if we are particularly interested in enhancing the accuracy of the reconstructed far-field radiation pattern in the region of the main and secondary lobes. In this case, the minimization of the functional is more effective by applying the constraints added by the Fourier Iterative Algorithm in each iteration so that the Global Optimization based on Genetic Algorithm speeds up the convergence on finding a suitable estimation of the field over the antenna aperture.

5.4 The problem of the twin images.

When applying exclusively Fourier Iterative Algorithm separately, it is appreciable to see that in different iterations we obtain different phases. For example, for the X-Component of the field over the 1st scanning plane, the phase distribution that we are looking for is as follows:

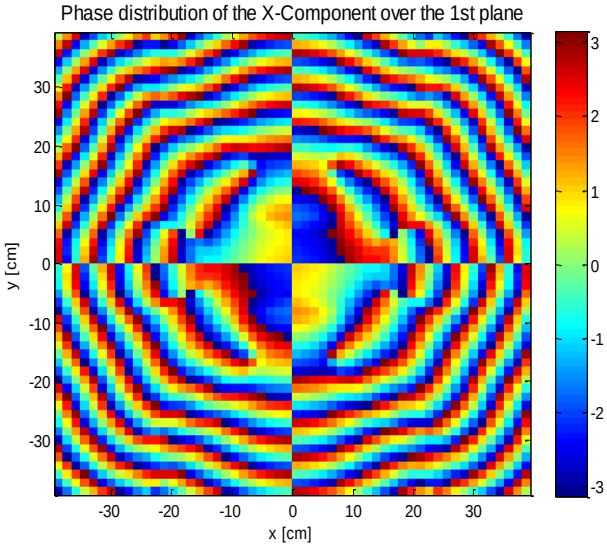

Figure 68: Phase distribution of the X-component of the field over the 1st plane

In Figure 69 the two possible features we are obtaining are shown after applying the Fourier Iterative Algorithm with 500 iterations:

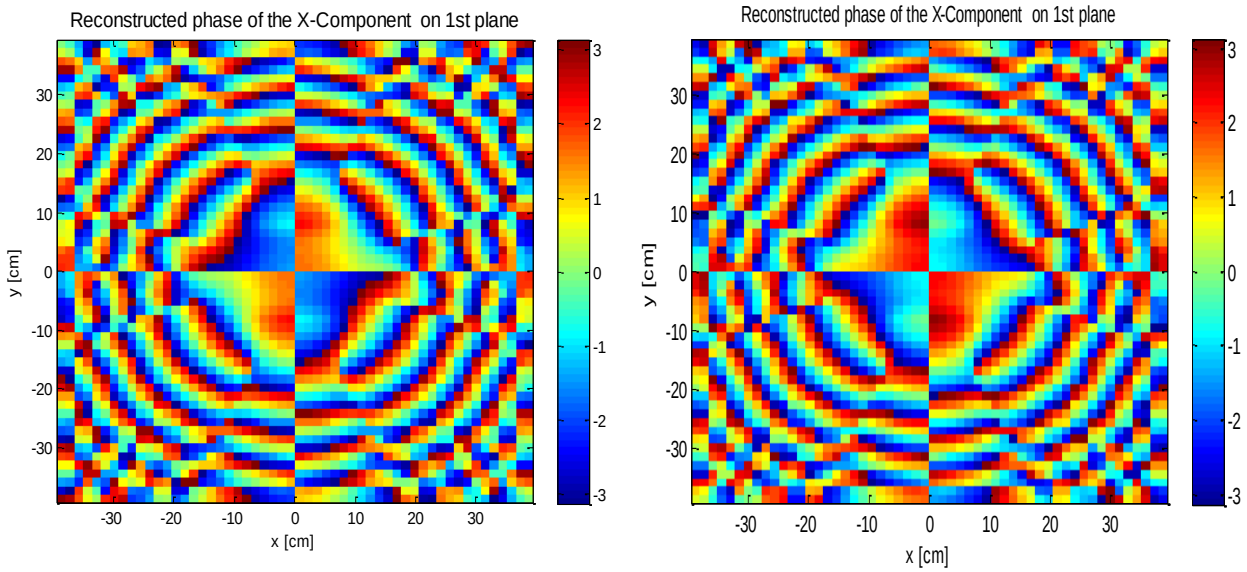

Figure 69: Twin phase distributions of the X-Component over the 1st plane

Basically, we are dealing with the problem of the twin images. This problem was addressed in Chapter 3, in Section 3.4 and in other documents of the literature [21].

For this particular antenna, this is not a problem. By increasing the number of iterations, finally FIA reconstructs one of the possible twin phase distributions. It was shown that in any case we had problems with stagnation of the Fourier Iterative Algorithm. Even though the problem of the twin phases does not hurt us due to the antenna we have chosen, the reduced-area support constraint method (which was addressed in Chapter 3 section 3.4.2) is applied when FIA is used alone or for the second method of the phase retrieval problem. By applying this constraint during the first iterations of the iterative technique, we always reconstruct the same feature of the phase distribution. In Figure 70, two simulations of the Fourier Iterative Algorithm with the reduced-area support constraint are shown and, as we can see, the reconstructed phase for both of them follows the same pattern:

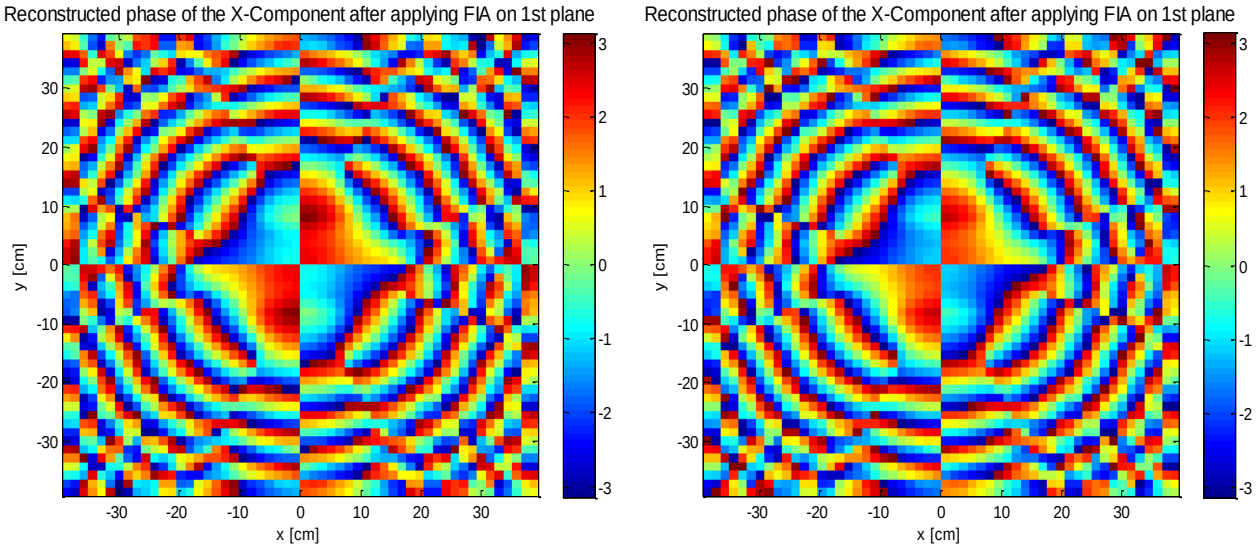

Figure 70: Different simulations of the reconstructed phase for the X-Component using the reduced-area support constraint

On the other hand, by applying the Global Optimization to find an initial guess of the field, we are forcing the Fourier Iterative Algorithm to bet for one of the possible solutions. That means that the Fourier Iterative Algorithm reconstructs a phase distribution following the initial estimation of the phase given by the Global Optimization, as we can see in Figure 71:

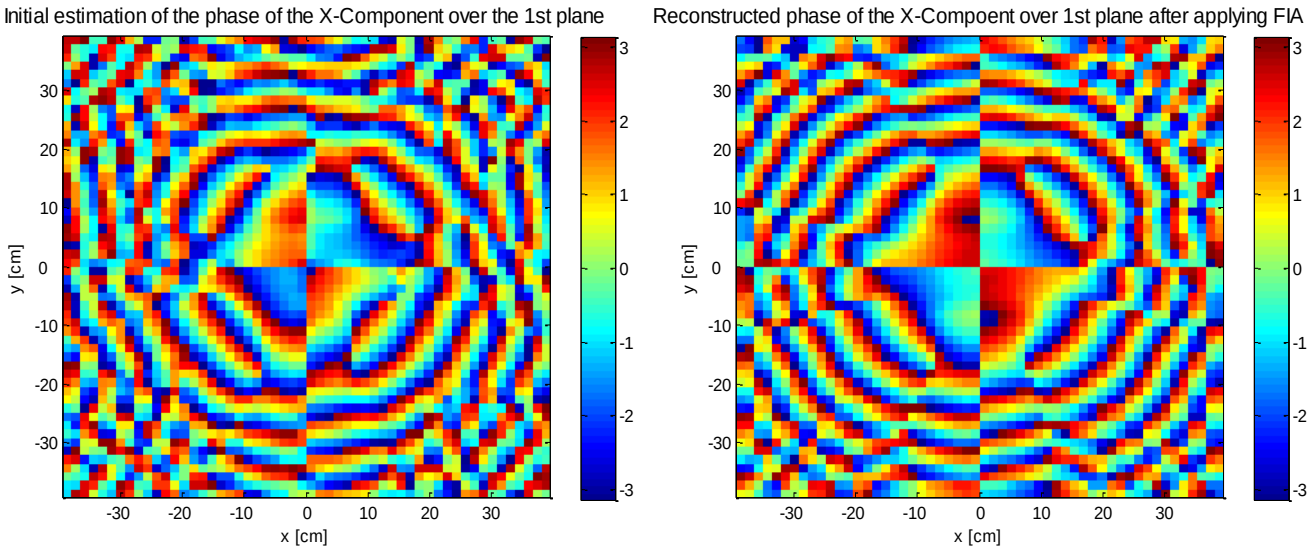

Figure 71: Reconstructed phase using GO+FIA after 50 iterations of FIA over 1st plane. Left: Initial estimation of the phase after using GO. Right: Final estimation of the phase after using FIA

In the previous figures, the left image is the reconstruction of an initial estimation of the phase over the first scanning plane and the second one is the final estimation of the phase over the same plane after applying FIA. As we can see, the simulations are according to the theoretical ideas, and the initial estimation compels the iterative technique to reconstruct one of the possible features in contempt to the other.

Although the problem of twin images is not such a problem for this particular antenna, it can be a problem for other antennas, and the solutions that have been raised here, the reduced-area constraint and the use of the Global Optimization to find the initial estimation of the phase, could be suitable solutions in those cases.

5.5 The reconstruction of the far-field from amplitude only data using one single scanning plane

During the development of this thesis, two scanning planes with amplitude measurements have been used to reconstruct the phase distribution of the near-field in order to acquire a complex near-field and the transformation to the far-field region can be carried out successfully. Nevertheless, the possibility of using one single scanning plane has been approached as well.

Different tests have been performed by using just one single scanning plane to reconstruct the near-field phase. The plane is located at 3λ and it conserves the dimensions and sample spacing of the previous two scanning planes. The architecture is shown in Figure 72:

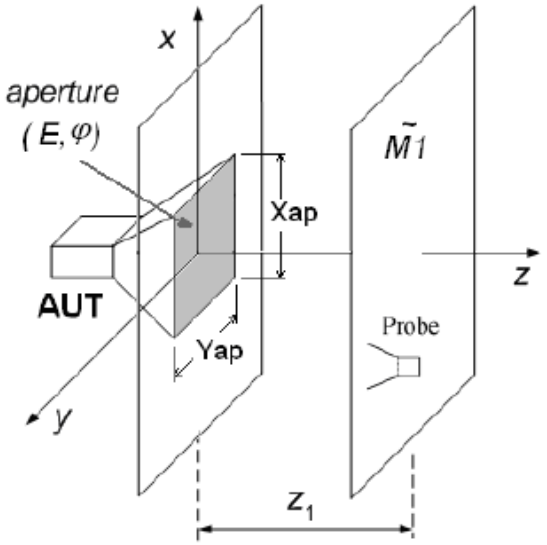

Figure 72: Architecture of the phase retrieval method with one scanning plane [Reconstruction of the near-field, Jan Puskely]

The implementation of the algorithms is similar, but we eliminate the contribution of the second scanning plane. We can still reconstruct an approximation of the phase distribution in the near-field, but of course this phase reconstruction is worse. Therefore, the reconstruction of the far-field radiation pattern will be less accurate, as we can see in Figure 73 and Figure 74.

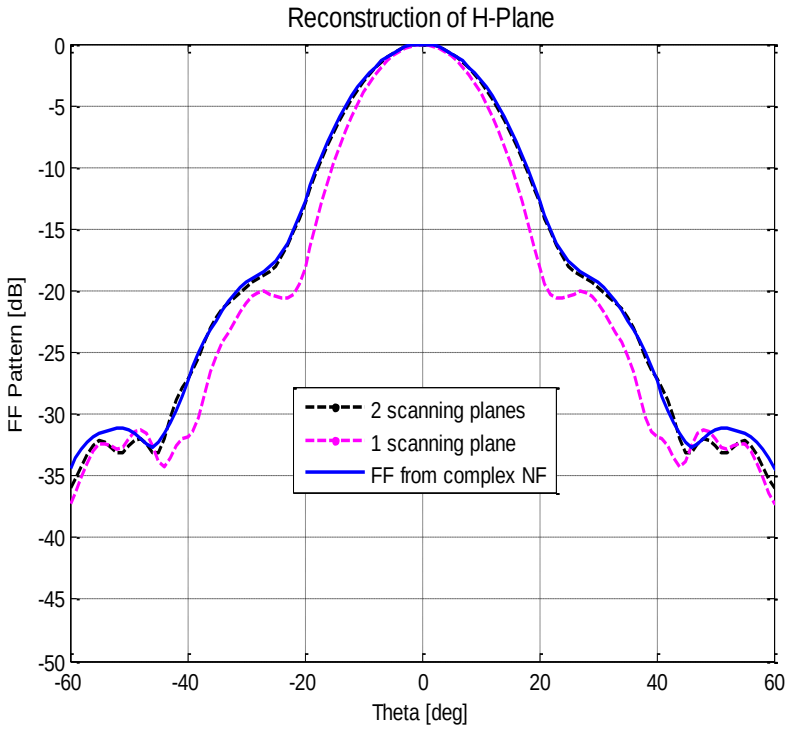

Figure 73: Comparison of the reconstruction of H-Plane using one and two scanning planes

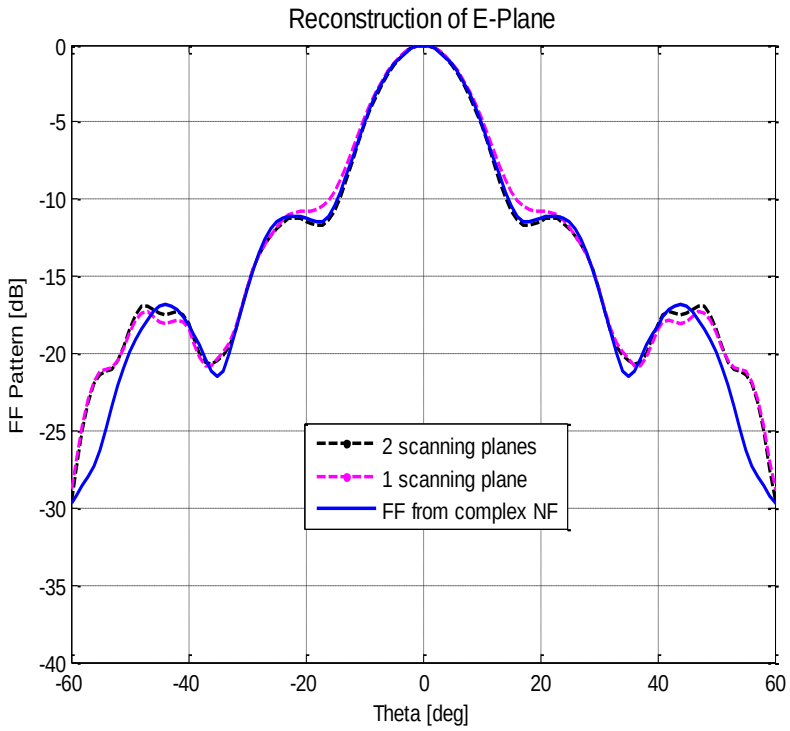

Figure 74: Comparison of the reconstruction of E-Plane using one and two scanning planes

In the following Figures, the error in both main planes of the far-field is shown.

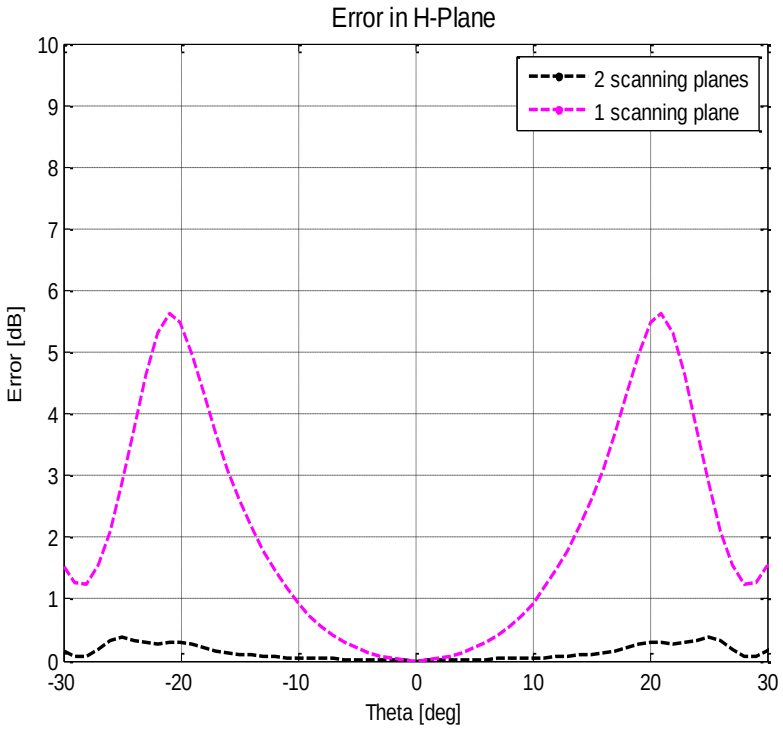

Figure 75: Error in H-Plane using one and two scanning planes

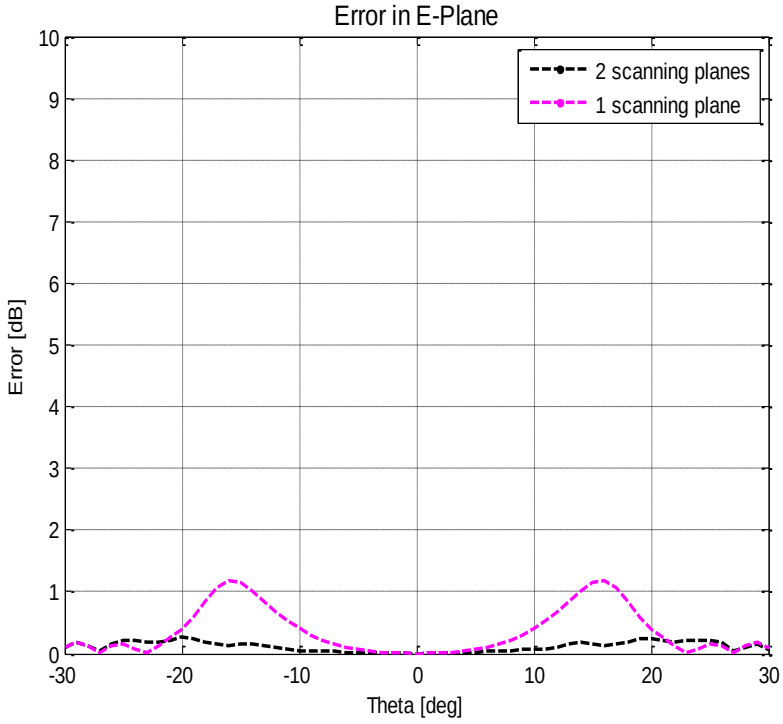

Figure 76: Error in E-Plane using one and two scanning planes

6 Conclusions

During the development of this thesis, the goal has been to reconstruct the far-field radiation pattern of an antenna from amplitude only near-field measurements. Different phase retrieval techniques have been investigated and developed in order to reconstruct the phase distribution from the amplitude measurements taken over planar scanning surfaces in the near-field region and all of them are based on the minimization of a cost function. The Fourier Iterative Algorithm has been used to reconstruct the phase from the amplitude data taken over two scanning planes but the problem of the dependence with the initial guess has been commented.

In order to avoid problems with the stagnation of the Fourier technique owning to the initial guess of the field over the antenna aperture, two different methods have been implemented, both of them based on a Global Optimization technique that implements a Genetic Algorithm and the accuracy of the reconstructed far-field radiation pattern has been evaluated. The first method implements the Global Optimization based on the Genetic Algorithm in order to find an initial guess of the field over the antenna aperture. With this initial guess the Fourier Iterative Algorithm is fed and refines the estimation of the phase. With the second method, the Global Optimization based on the Genetic Algorithm and the Fourier Iterative Algorithm are implemented in the same algorithm to find an estimation of the complex near-field. The Genetic Algorithm generates in each iteration an initial estimation of the field over the antenna aperture. This estimation is refined by applying an iteration of the Fourier Iterative Algorithm, until the suitable estimation of the complex near-field is found.

According to the results obtained with the Horn antenna, the Fourier Iterative Algorithm works really well with any kind of initial distribution of the field over the antenna aperture, and after some iterations, the algorithm reconstructs a suitable estimation of the phase distribution from the amplitude data. In this particular case, the application of the Global Optimization based on a Genetic Algorithm does not help to enhance the accuracy of the reconstructed far-field radiation pattern respect the use of the iterative technique by itself. Therefore, it seems to be that, for this particular antenna, whose radiation pattern is not really complex, the Fourier Iterative Technique offers a straightforward method to reconstruct with a great level of accuracy the far-field radiation pattern without problems and without the necessity of using a global optimization procedure to find an initial guess of the field.

On the other hand, for the second phase retrieval method, the results show that, in the region of the main and the side lobes, this hybrid solution achieves a better level of accuracy than using exclusively the Fourier Iterative Algorithm or using the Global Optimization to find the initial guess of the field with which the Fourier Iterative Algorithm is fed. We can conclude with this that, if we use the Fourier Iterative Technique in each iteration to add a constraint over the estimation of the field over the antenna aperture, the algorithm is helping the Genetic

Algorithm to speeds up the convergence and, furthermore, the reconstruction of the estimation of the near-field is going to be better.

On the other hands, other issues have been studied. In the case of the stagnation problem due to the twin images of a same phase distribution, we conclude that the Fourier Iterative Algorithm does not have problems of stagnation for this particular antenna, so that when the number of iterations increases, the algorithm always reconstructs one of the possible features of the phase. On the other hand, the reduced-area support constraint has been found suitable to avoid the problem of the twin images and has been applied. The results of the simulation show that by applying this technique, we always get the same feature of the phase, so that we conclude this technique could solve the problem of stagnation for other antennas. Apart from that, the simulations also show that, if the Global Optimization is applied previously to the Fourier Iterative Algorithm to get an initial estimation of the field over the antenna aperture, the Fourier Iterative Algorithm refines the initial estimation of the phase, hence the problem of the twin images disappears.

Finally, some simulations using one single scanning plane were made. The simulations show that, in terms of accuracy of the reconstructed far-field radiation pattern, it is worthy to use two sets of measurements, since the lack of information we have with only one single scanning plane produces more inaccuracy in the estimation of the phase of the near-field and, consequently, in the reconstruction of the far-field.

7 Future Work

After being working on the topic of this project, some future work is proposed to keep on investigating the reconstruction of the far-field radiation pattern from phaseless near-field measurements.

It would be pretty interesting to check the programmed codes with other kind of antennas. As it has been explained, the antenna which has been analyzed has been the Horn antenna. It would be interesting to check the present results for other antennas, especially high-directive antennas, in order to see if the conclusions that have been reached can be generalized for a particular group of antennas or these conclusions only can be applied to the Horn antenna.

Apart from that, it would be interesting to develop a time analysis of the algorithm efficiency and to try to enhance the speed of convergence of this algorithm. During the development of this project we have been more focused on the enhancement of the accuracy of the reconstructed far-field radiation pattern. However, we cannot forget the importance of the time efficiency in the industry, so that we conclude that a time efficiency analysis of the code and the efforts to improve the time efficiency of the whole system would be suitable.

List of Figures

Figure 1: Exterior fields of a radiating antenna [*Reconstruction of the antenna near-field* Jan Puskely, Figure 1.1] 7
Figure 2: Procedure to reconstruct the far-field from complex near-field measurements. 8
Figure 3: General procedure to reconstruct the Far-Field from near-field amplitude only measurements. 8
Figure 4: Standard scanning surfaces used in near-field antenna measurements [Principles of Planar Near-Field Antenna Measurements, Stuart Gregson, John McCornick and Clive Parini] 10
Figure 5: Geometry of planar near-field measurement [An examination of the theory and practices of Planar Near-Field Measurements, Johnson J.H. Wang] 11
Figure 6: Different configuration for the planar measurement system [Principles of planar near-field antenna measurements, Stuart Gregson, Jon McCorcnick and Clive Parini, Figure 3.10]. 11
Figure 7: Architecture of the rectilinear scanning plane. [An examination of the theory and practices of Planar Near-Field Measurements, Johnson J.H. Wang] 12
Figure 8: Flow-Chart of the NF-FF transformation. 14
Figure 9: Reconstruction of the FF in H-Plane 15
Figure 10: Reconstruction of the FF in E-Plane 15
Figure 11: The valid angle of the planar near-field antenna measurements [Principles of planar near-field antenna measurements, Stuart Gregson, Jon McCorcnick and Clive Parini, Figure 5.2] 16
Figure 12: Planar Near-Field Antenna Measurements architecture to take amplitude data [Reconstruction of the Near-Field, Doctoral Thesis, Jan Puskely, Figure 2.1] 17
Figure 13: Classification of the Functional Minimization Methods. 18
Figure 14: Cost function surface 19
Figure 15: Hill-Climbing with search domain between 0 and 4 20
Figure 16: Hill-Climbing with search domain between 0 and 8 20
Figure 17: Flow Char of the classical Fourier Iterative Algorithm. 21
Figure 18: Procedure to reconstruct the phase from only amplitude data in the near-field. 23
Figure 19: Flow Char of the first version of Global Optimization 24
Figure 20: Schematic representation of the first version of the Global Optimization procedure [Reconstruction of the antenna near-field, Jan Puskely, Figure 3.17] 25
Figure 21: Global Optimization based on the principle of Fourier Iterative Algorithm 26
Figure 22: Schematic representation of the second version of GO 27
Figure 23: Example of the simultaneous twin-images problem [Phase-retrieval stagnation problems and solutions, J.R.Fienup and C.C.Wackerman]. 29
Figure 24: Reduced-area support constraint and total area constraint for the antenna aperture 30
Figure 25: Classification of Genetic Algorithms. 31
Figure 26: Flow Char of a generic Genetic Algorithm. 32
Figure 27: Natural Selection in Genetic Algorithms [Practical Genetic Algorithms, Randy L. Haupt, Sue Ellen Haupt, Figure 2.9] 33
Figure 28: One single crossover point [Wikipedia: Crossover in Genetic Algorithms] 34
Figure 29: Two crossover points [Wikipedia: Crossover in Genetic Algorithms] 34
Figure 30: Example of mutation in the Binary Genetic Algorithm 35
Figure 31: Example of crossover and mutation in the Real Valued Genetic Algorithm 35
Figure 32: Relationship between the Genetic Algorithm concepts and the problem of Phase Retrieval 36

Figure 33: Factors to take into account when programming the initial population in GA 37
Figure 34: Selection of the 50% best individuals 38
Figure 35: Tournament Selection 39
Figure 36: Initial Population of the Genetic Algorithm 41
Figure 37: State of the population after 20 iterations 42
Figure 38: State of the population after 50 iterations. 42
Figure 39: State of the population after 100 iterations 43
Figure 40: Scheme of the Horn antenna to characterize 44
Figure 41: Amplitude distributions over the 1st scanning plane 45
Figure 42: Amplitude distributions over the 2nd scanning plane 45
Figure 43: H-Plane and E-Plane of the far-field 46
Figure 44: Convergence of Global Optimization for 10.000 iterations. 47
Figure 45: Reconstructed amplitude for the X-Component over the 1st plane 48
Figure 46: Reconstructed amplitude for the Y-Component over the 1st plane 48
Figure 47: Initial estimation of the phase over the 1st plane for the X-Component 49
Figure 48: Initial estimation of the phase over the 1st plane for the Y-Component 49
Figure 49: Convergence of the Fourier Iterative Algorithm 50
Figure 50: Reconstruction of the H-Plane 51
Figure 51: Reconstruction of the E-Plane 51
Figure 52: Error in main planes, H-Plane and E-Plane 52
Figure 53: Comparison between using only FIA or FIA+GO when increasing the number of iterations of FIA. 53
Figure 54: The asymmetry of the reconstructed far-field radiation pattern. 54
Figure 55: Convergence speed of the Global Optimization for different population sizes. 55
Figure 56: Convergence speed of Global Optimization for different mating strategies. 56
Figure 57: Convergence of Global Optimization for different crossover rates. 56
Figure 58: Convergence of Global Optimization for different β-parameters 57
Figure 59: Convergence of the Global Optimization for different mutations rates. 58
Figure 60: Error in E-Plane for different crossover rates. Left: FIA has 50 iterations. Right: FIA has 500 iterations. 59
Figure 61: Error in E-Plane for different mutation rates. Left: FIA has 50 iterations. Right: FIA has 500 iterations. 59
Figure 62: Comparison of the convergence between the first method of phase retrieval and the second method. 60
Figure 63: Comparison of the accuracy in the far-field with the first method of phase retrieval and the second method. 61
Figure 64: Reconstruction of the amplitude of the X-component over the 1st plane 61
Figure 65: Reconstruction of the amplitude of the Y-component over the 1st plane 62
Figure 66: Comparison of the error in the valid region between using FIA and the second phase retrieval method 63
Figure 67: Comparison of the accuracy of the far-field between hybrid method and using only FIA. 63
Figure 68: Phase distribution of the X-component of the field over the 1st plane 64
Figure 69: Twin phase distributions of the X-Component over the 1st plane 64
Figure 70: Different simulations of the reconstructed phase for the X-Component using the reduced-area support constraint 65
Figure 71: Reconstructed phase using GO+FIA after 50 iterations of FIA over 1st plane. Left: Initial estimation of the phase after using GO. Right: Final estimation of the phase after using FIA 66

Figure 72: Architecture of the phase retrieval method with one scanning plane [Reconstruction of the near-field, Jan Puskely]..... 67
Figure 73: Comparison of the reconstruction of H-Plane using one and two scanning planes..... 68
Figure 74: Comparison of the reconstruction of E-Plane using one and two scanning planes 68
Figure 75: Error in H-Plane using one and two scanning planes..... 69
Figure 76: Error in E-Plane using one and two scanning planes 69

Bibliography

[1] *Antenna Theory: Analysis and Design* [Constantine A. Ballanis].

[2] *Principles of Planar-Near-field Antenna Measurements* [Stuart Gregson, John McCornickand Clive Parini].

[3] *Practical Genetic Algorithms* [Randy L.Haupt, Sue Ellen Haupt].

[4] *Reconstruction of the antenna near-field* [Jan Puskely].

[5] *Using Global Optimization Approaches to Reconstruct Radiation Patterns* [Jan Puskely]

[6] *Recent Developments in evolutionary and Genetic Algorithms: Theory and Applications* [N. Chaiyarataa and A.M.S. Zarzala]

[7] *Performance Evaluation of Phase Retrieval Method based on amplitude-only Near-Field Data* [Markus Johansson, Hoi-Shun Lui, Mikael Persson]

[8] *Signal Reconstruction from Phase and Magnitude* [Monson H.Hayes, Jae S.Lim and Alan V.Oppemheim]

[9] *Comparison of Different Heuristic Optimization Methods for Near-Field Antenna Measurements* [Jesus Ramon Perez and Jose Basterrechea]

[10] *New Look to Real Valued Genetic Algorithm Used to Reconstruct Radiation Patterns* [Jan Puskely]

[11] *A Direct Optimization Approach for Source Reconstruction and NF-FF transformation using only Amplitude-Only Data* [Fernando Las-Heras and Tapan K.Sarkar]

[12] *Comparison between Genetic Algorithms and Particle Swarm Optimization* [Rusell C.Eberhart and Yuhui Shi]

[13] *Improving the Performance of Genetic Algorothm by reducing the Population Size* [Vishnu Raja.P., Murali Bhaskaran.V.]

[14] *Genetic Algorithms: A Survey* [M.Srinivas, Motorola India Electronics]

[15]*Mechanisms to Avoid the Premature Convergence of Genetic Algorithms* [Elena Simona Nicoara]

[16]*Adaptive Probabilities of Crossover and Mutation in Genetic Algorithms* [M. Srinivas and L.M. Patnaik]

[17] *An Improved Fast-Convergence Genetic Algorithm* [WEI Gao]

[18] *An Examination of the Thery and Practises of Planar Near-Field Measurements* [Johnson J.H.Wang]

[19] *Local Search and Optimization, Chapter 4* [Mausam, (Based on the slides of Padhraic Smyth, Stuart Russell, Rao Kambhampati, Raj Rao, Dan Weld)]

[20] *Empirical study: Initial Population Diversity and Genetic Algorithm Performance* [Pedro A.Díaz Gómez and Dean F.Hougen]

[21] *Phase retrieval stagnation problems and solutions* [J.R.Fienup, C.C. Wackerman]

[22]*Comparison between Genetic Algorithms and Particle Swarm Optimization* [Russell C.Eberheart and Yuhui Shi]

[24] *An effective near-field far-field transformation technique from truncated and Inaccurate Amplitude-Only Data* [Ovidio M.Bucci, Giuseppe D,Ella and Marco Donald Migliore]